Tectonophysics, 136 (1987) 27–63
Elsevier Science Publishers B.V., Amsterdam – Printed in The Netherlands

Flow properties of continental lithosphere

NEVILLE L. CARTER and MICHAEL C. TSENN

Center for Tectonophysics, Texas A & M University, College Station, TX 77843 (U.S.A.)

(Accepted December 1, 1986)

Abstract

Carter, N.L. and Tsenn, M.C., 1987. Flow properties of continental lithosphere. *Tectonophysics*, 136: 27–63.

The occurrence of mechanically weak zones ($\sigma_1 - \sigma_3 < 10$ MPa) at upper-, mid- and lower crustal depths, inferred from geological and geophysical observations and interpretations, is supported by empirically-determined steady-state flow properties of some common crystalline rocks. These zones are predicted to occur in the depth intervals 10–15 km, 20–28 km and 25–40 km, these intervals depending critically on rock type and tectonic province. In addition, the apparent widespread occurrence of ductile and semi-brittle fault zones suggests that weak zones may occur at virtually any depth below about 10 km. While data are not available for representative lower crustal materials, those likely to be closest in mechanical response support the common suggestion that the Moho is a mechanical discontinuity, with stronger peridotite below, but the magnitude of the discontinuity is shown to depend critically on temperature and strain rate.

Mantle flow is currently best approximated by Chopra and Paterson's (1981, 1984) wet Aheim dunite flow law. Combined with pyroxene thermobarometry and olivine paleopiezometry of mantle xenoliths, the wet flow law permits construction of viscosity–depth profiles that are in accord with other geophysical considerations. Yield envelopes commonly applied to geological and geophysical problems since the original one proposed for the lithosphere and upper asthenosphere by Goetze and Evans (1979) generally lead to serious overestimates of stress differences because of extrapolations both of Byerlee's (1978) rock-friction relation and of steady-state flow laws to physical conditions beyond their range of validity. Modifications of the envelopes, will require careful additional experimental work on rock friction along with detailed delineations of boundaries between brittle, semi-brittle and ductile regimes, grainsize-sensitive domains, and their depth-dependencies. Once accomplished, realistic yield envelopes and refined deformation surfaces will lead to a much better understanding of the mechanical behavior and governing flow processes at depth in the continental lithosphere.

Introduction

A recently published symposium on "Collision Tectonics: Deformation of Continental Lithosphere" (Carter and Uyeda, 1985) presents our current understanding of this important but exceedingly complex topic and poses many problems amenable to solution by keen perceptions and well-conceived future research. One of these, summarized by Kirby (1985), is the flow properties and processes of some important rocks, primarily silicates, forming the continental lithosphere, as determined by laboratory experiments and by investigations of deformation processes in naturally deformed rocks. It is the intent of this paper to explore this topic in more detail than was possible in Kirby's general treatment and to present our perceptions of the flow properties of continental lithosphere, some of which differ significantly from those of Kirby (1985). As such, the paper is by no means a review of the topic, but merely an analysis of selected pertinent information, interpretations of their significance as applied to this problem, and suggestions for future research in this general area.

Constitution and physical environment of continental lithosphere

The mechanical behavior and flow processes of continental lithospheric rocks depend critically on the depth-dependent physical/chemical environment. This problem is exceedingly complex because of: (1) the differing tectonic provinces involved with a wide variety of structures, environments and lithologies, all of which are poorly-constrained at depth; and (2) our increasing but still crude understanding of the depth- and time-dependent rheology of even the most common crustal rocks. The block diagram of Fig. 1 illustrates an imagined section through the continental crust, along with representative lithostatic pressure, temperature, metamorphic grade and dominant deformation mechanisms.

Constitution

Recognizing the heterogeneities and complexities inherent in constructing even a simple representative continental lithospheric crustal model, we are in general agreement with the observations and views of some other investigators including Smithson and Brown (1977), Fountain and Salisbury (1981), Kay and Kay (1981), Sibson (1984) and Brodie and Rutter (1985, 1987). A layer of sediments of diagenetic and low-grade (zeolite–

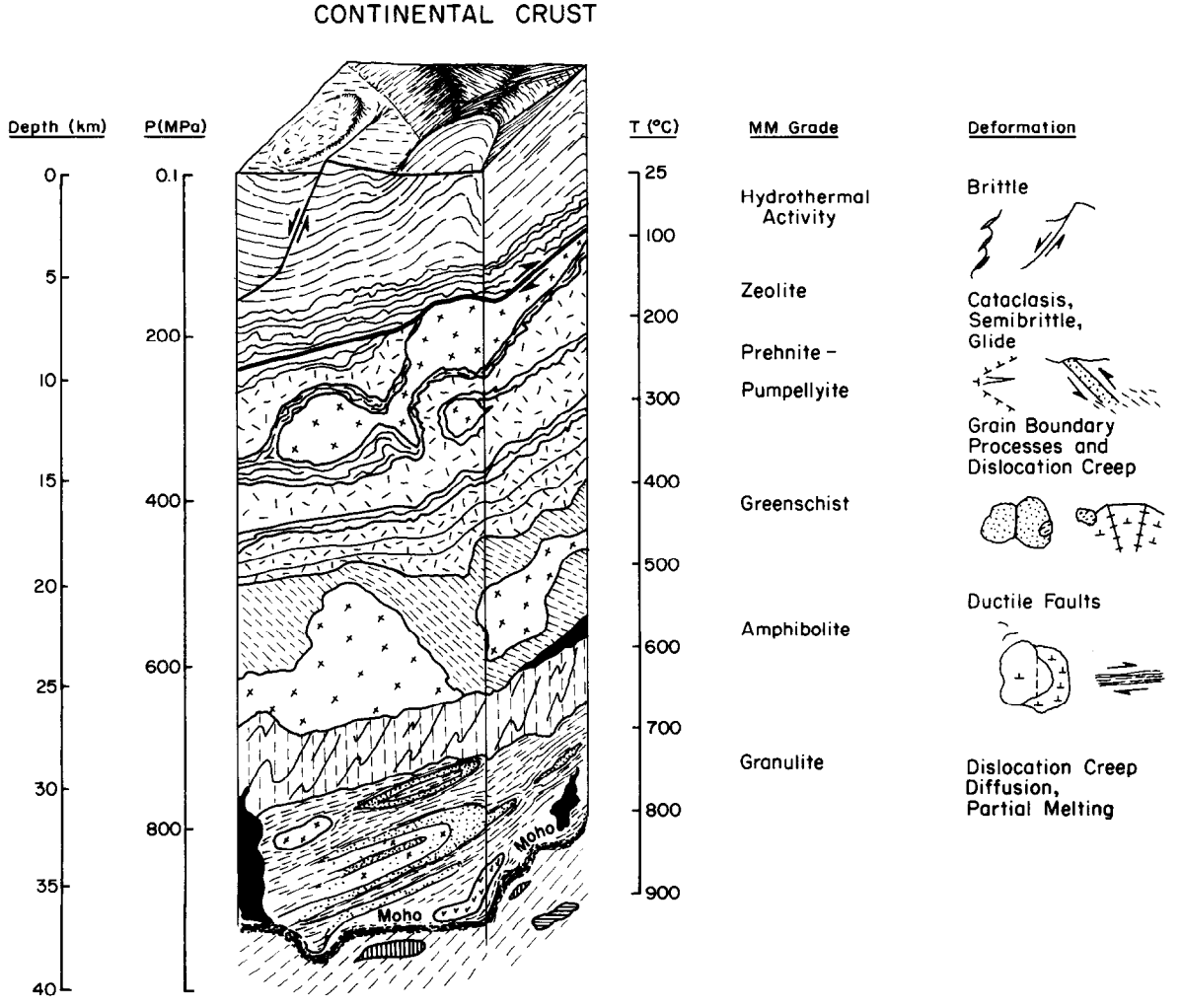

Fig. 1. Idealized block diagram showing imagined continental crustal structure, along with lithostatic pressure (26 MPa/km), temperature (25°C/km), metamorphic grade and dominant deformation mechanisms.

pumpellyite) facies progresses downward to greenschist facies assemblages. At midcrustal depths silicic to intermediate composition materials of amphibolite facies metamorphism prevail, associated with local granite plutonism and migmatization. At lower crustal depths, mafic to intermediate composition rocks of granulite grade dominate and these rocks are commonly associated with silicic gneisses and mafic to intermediate composition plutonic bodies. This general progressive crustal sequence, about 35–40 km thick, rests on dominantly ultramafic upper mantle material (e.g., Clark and Ringwood, 1964; Carter et al., 1972; Mercier and Nicolas, 1975; Nicolas and Poirier, 1976; Avé Lallemant et al., 1980; Weidner, 1985), which persists throughout the mechanical lithosphere to an appreciable depth below, and is composed primarily of olivine with lesser quantities of pyroxenes and other aluminous phases and accessories. Thus, ignoring sediments, data available for marble, quartzite, and granite may reflect the upper crustal mechanical response to the physical environment, and the rheologies of granodioritic, feldspathic and dioritic rocks, the midcrustal response. The greatest need is for information on the rheology of a representative lower crustal material, such as a pyroxene–amphibole–plagioclase granulite. Data for orthopyroxenites, websterites and clinopyroxenites only are currently available; these materials are present both in the crust and upper mantle. Extensive analyses of flow properties of olivine and peridotites should represent the mechanical response of the upper mantle at high temperature adequately, but data at low to moderate temperatures are sparse.

Temperature

For the depth-dependence of temperature in orogenic and cratonic regions, we use Mercier's (1980a) equations for oceanic and continental geotherms, respectively. These equations, adjusted for pressure in MPa and for a temperature of 25°C at the surface (Table 1) are based on pyroxene thermobarometry of peridotite mantle xenoliths and permit temperature estimates below 40 km. Averaged temperatures estimated for the continents yield a geotherm of 16°C/km to 40 km, agreeing with the 16°C/km value obtained by Lachenbruch and Sass (1977) for stable cratons (1.3 HFU) and the 20°C/km estimate for the oceanic geotherm compares reasonably well with their 22°C/km for the Basin and Range (1.7 HFU). Mercier's continental geotherm corresponds closely to that of Clark and Ringwood (1.5 HFU) to 200 km and the oceanic geotherm to that of Griggs (1972) to 150 km, both based on theoretical considerations. While it is recognized that thermal regimes range widely both within and between tectonic provinces (Guffanti and Nathenson, 1980), average values of 16°C and 20°C/km are regarded as satisfactory estimates for cratons and certain orogenic regions, respectively.

Pressure

Estimates of lithostatic pressure ($P_l = \rho g z$) are somewhat model- and province-dependent because of variations in the density distributions assumed. However, average values of 26 MPa/km for the crust and 33 MPa/km for the upper mantle are probably representative to $\pm 10\%$.

Much less certain are estimates of effective pressure ($P_e = P_l - P_p$) because of the paucity of pore-pressure (P_p) data except at relatively shallow depths in certain sedimentary basins of economic interest. The need to specify P_p is extremely important (e.g., Handin et al., 1963; Brace, 1972, 1980, 1984; Brace and Kohlstedt, 1980; Etheridge et al., 1984). The key factor is permeability which, if sufficiently low, will favor high P_p and hence low P_e, reducing fracture and frictional strengths and favoring brittle behavior if the effect is purely mechanical. However, the effect of high pore pressure at depth may be chemical as well, enhancing ductility by hydrolytic weakening, pressure solution, intergranular mass transport and a variety of other processes.

Brace and Kohlstedt (1980) conclude that there is compelling evidence for pore and/or fracture interconnection to 5 km, good arguments for interconnection to a depth of 8 km and a suggestion that transmissivity might be appreciable to 20 km or so. Fyfe et al. (1978) present evidence for fluid pressures approximately equal to lithostatic pres-

TABLE 1

Temperature—continental lithosphere (40 km)

Determination	Result	Source
Temperature/depth measurements		
U.S. (> 600 m holes)	15–37 °C/km	Guffanti and Nathenson (1980)
Conductive geotherms (heat flow measurements)		
Stable Craton (1.3 HFU)	16 °C/km	Lachenbruch and Sass (1977)
Basin and Range (1.7 HFU)	22 °C/km	
Mantle xenolithes—pyroxene thermobarometry		
Continental:		
$T = 888 + 0.09(P + 780) - 7.3 \times 10^5/(P + 780)$	16 °C/km	Mercier (1980a)
Oceanic:		
$T = 1.9 \times 10^3 + 8.5 \times 10^{-3}[P + 1480] - 2.8 \times 10^6/(P + 1480)$	20 °C/km	

sure over broad regions of low to medium grade metamorphism. Etheridge et al. (1984) show that pore fluid pressures during regional metamorphism, even at moderate to high temperatures, generally exceed the minimum principal compressive stress, leading to relatively high porosities and permeabilities. Kerrich et al. (1984) demonstrate fluid participation in deep (> 15 km) fault zones primarily from $^{18}O/^{16}O$ relations. Similarly, Taylor's (1977) isotopic studies of granitic batholiths indicate that meteoric waters can penetrate depths to 20 km. Shimamoto (1985a) argues for abundant H_2O and restricted regions of abnormal pore pressures during progressive metamorphism to 25 km based on low seismicity and tectonic stress, inter-plate decoupling and ductile deformation in shallow subducting plates. Thus, there is mounting evidence for the general availability of H_2O during deformation and metamorphism of large volumes of continental crust and that regions of abnormally high (above hydrostatic) pore fluid pressures are fairly common. This conclusion bears heavily on the nature of deformation at depth and on the magnitude of deviatoric stresses responsible for it.

Strain rate

Strain rates are also expected to vary widely both with depth and tectonic province (Table 2). Estimates of strain rates have been derived from geodetic measurements of surface displacements, such as those along the San Andreas fault (Whitten, 1956), those due to rebound from ancient water and ice loads (e.g., Haskell, 1935; Crittenden, 1967; McConnell, 1968; Walcott, 1970; Cathles, 1975) and estimated rates of shortening in orogenic regions (Gilluly, 1972). These rates fall in the range 10^{-13} to 10^{-15} s^{-1} and are in accord with strain rates determined from analyses of 990 slates (Ramsay and Wood, 1973) and from deformations of naturally deformed objects in young orogenic regions (Pfiffner and Ramsay, 1982). However, Sibson (1977, 1982, 1983, 1984) has suggested that strain rates along mylonite zones and parts of the San Andreas may be as high as 10^{-10} s^{-1} and average values nearer 10^{-17} s^{-1} may be more appropriate to small strains associated with flexures and other deformations in oceanic lithosphere (e.g., McNutt, 1980; Kirby, 1983). Mercier et al. (1977), Mercier (1980b) and Avé Lallemant et al. (1980) show that the strain rate in the upper mantle beneath South Africa generally increases from about 10^{-17} s^{-1} at 75 km depth to about 10^{-12} s^{-1} at 250 km. Recognizing these wide variations, and occurrences of very high local instantaneous strain rates, it is necessary to adopt representative values of average strain rates primarily for comparisons of flow stress with depth of the several continental lithospheric materials analyzed below. According, we have selected an average strain rate of 10^{-14} s^{-1} for orogenic regions and 10^{-15} s^{-1} for cratonic lithosphere.

TABLE 2

Pressure and strain rate—continental lithosphere

Parameter	Determination	Result	Source
Lithostatic pressure	$P_l = \rho g h$	~ 26 MPa/km crust ~ 33 MPa/km mantle	
Effective pressure	$P_e = P_l$(dry), $P_e = 0.63P_l$ (hydrostatic), $P_e \to 0$, $\lambda \to 1$		
Strain rate	surface displacements		
	San Andreas Fault	10^{-14} s^{-1}	Whitten (1956)
	isostatic rebound,		
	water and ice	10^{-13}–10^{-15} s^{-1}	Haskell (1935) Crittenden (1967) McConnell (1968) Walcott (1970) Cathles (1975)
	shortening in orogenic regions	10^{-14}–10^{-15} s^{-1}	Gilluly (1972)
	strain in 990 slates	10^{-14} s^{-1}	Ramsay and Wood (1973)
	deformation of natural objects	10^{-13} s^{-1}	Pfiffner and Ramsay (1982)
	extension—Basin and Range	10^{-15} s^{-1}	Fletcher and Hallet (1983)
	shear in fault and mylonite zones	10^{-10}–10^{-12} s^{-1}	Sibson (1977, 1982, 1983, 1984) Pfiffner and Ramsay (1982)
	upper mantle olivine grainsize		
	South Africa	10^{-12}–10^{-17} s^{-1}	Mercier (1980b)
	Basin and Range	10^{-15}–10^{-17} s^{-1}	Avé Lallemant et al. (1980)

Stress

The magnitude of deviatoric stress in the upper part of the earth bears so heavily on all aspects of tectonophysics and geodynamics that Hanks and Raleigh (1980) convened and published the results of a conference limited to this topic. Arguments were presented in support of high as well as low average shear stresses (from 1 to 150 MPa), based on global and regional geophysical, geodynamical, and rock-deformation observations and inferences. The diversity of opinion appears to reflect our ignorance of how geologic processes work on large scales for long times and the important effects of fluids under lithospheric conditions. We offer a brief discussion of these and more recent results (Table 3).

McGarr (1980) reviewed in situ stress determinations, made to a maximum depth of 5.1 km, in both soft (e.g., shale, sandstone) and hard (e.g., granite, quartzite) rocks in North America, southern Africa and Australia (see also compilation of 116 data sets by Hoek and Brown, 1980). While the data are scattered, the maximum shearing stress, $\tau_m = (\sigma_1 - \sigma_3)/2$, appears to increase linearly with depth with average gradients of 3.8 and 6.6 MPa/km for soft and hard rock, respectively. The hard-rock data of primary concern here extend to 3 km and the average maximum shearing stress for all 59 measurements may be restated as (McGarr, 1980):

$$\tau_m = 5.0 + 6.6z \qquad (1)$$

As pointed out by McGarr, a linear extrapolation of these direct determinations would be qualitatively consistent with the high deviatoric stresses predicted by Brace and Kohlstedt (1980) using Byerlee's (1968, 1978) relation for frictional sliding to a depth of 15 km.

Byerlee's relation which is based on, or consistent with, laboratory results on crystalline rocks deformed at pressures to 600 MPa, temperatures to about 200°C (Stesky et al., 1974) over a wide range of strain rates may be stated as:

$$\tau = 0.85\bar{\sigma}_n \qquad \bar{\sigma}_n < 200 \text{ MPa} \qquad (2a)$$

$$\tau = 60 + 0.6\bar{\sigma}_n \qquad 200 < \bar{\sigma}_n < 1700 \text{ MPa} \qquad (2b)$$

where τ is the shear stress necessary to overcome

TABLE 3

Stress—continental lithosphere

Determination	Result	Source
Laboratory		
Rock friction experiments	$\tau = 0.85\bar{\sigma}_n$, $\bar{\sigma}_n < 200$ MPa $\tau = 60 + 0.6\bar{\sigma}_n$, $\bar{\sigma}_n = 200$–1700 MPa	Byerlee (1968, 1978)
Application of friction experiments and flow laws		
Byerlee's relation and quartzite flow law—San Andreas	100 MPa (13 km)	Sibson (1984)
Byerlee's relation and granite flow law—San Andreas	150 MPa (18 km)	Sibson (1984)
Byerlee's relation and wet quartzite flow law—many faults	150 MPa (5–10 km)	Meissner and Strehlau (1982)
Paleopiezometers (Laboratory calibrated)		
Dolomite Twins		
Front Range Thrusts, Canada	62 MPa	Jamison and Spang (1976)
Moine Thrust, Scotland	> 100 MPa	Tullis (1980)
Clinopyroxenite Twins		
Palmer area fault, southern Australia	140 MPa	Tullis (1980)
Quartz, free dislocation density, subgrain and recrystallized grainsize		
Several major faults	10–100 MPa	Kohlstedt and Weathers (1980)
Mylonites from Moine Thrust, Scotland		
subgrain size		
Fault	75 MPa	
Regional	35 MPa	White (1979a, b)
Mylonites from Coyote Mountain, Calif.		
Recrystallized grainsize	8–37 MPa	Christie and Ord (1980)
Free dislocation densities	25–75 MPa	
Synclinorium, Marquette, Mich.		
Recrystallized grainsize	1–19 MPa	Kappmeyer and Wiltschko (1984)
Subgrain size	6–20 MPa	
Free dislocation densities	16–36 MPa	
Olivine—recrystallized grainsize		
Lanzo Massif, Italy	< 30–150 MPa	Mercier et al. (1977)
Upper mantle xenoliths	1–50 MPa	Mercier (1980b), Avé Lallemant et al. (1980)
Peridotites from 11 ophiolites		
Subgrains	1–90 MPa	Nicolas et al. (1980)
Recrystallized grains	1–100 MPa	
Calcite, free dislocation densities, subgrain size		
Intrahelvetic complex	42–100 MPa	Pfiffner (1982)
Glaurus mylonite	25–160 MPa	
Field observations and theory		
Hydrofracturing		
San Andreas granitic (to 1 km)	$\tau = 9.6$ MPa/km	Zoback et al. (1980)
Illinois granite (686–1449 m)	$\tau_m = 9.4Z$	Haimson and Doe (1983)
Worldwide crystalline rocks (to 3 km, other techniques also)	$\tau_m = 5.0 + 6.6Z$	McGarr (1980)
Wellbore breakouts		
Kola well at 11.6 km	< 150 MPa	Zoback and Mastin (1986)
Stresses in deep mines		
Rockbursts	~ 100 MPa	McGarr (1984)

TABLE 3 (continued)

Determination	Result	Source
Theoretical analyses-layered elastic crust		
Hydrofracturing and displacement measurements		
San Andreas Fault		
< 2 km	9 MPa/km	Leary (1985)
> 2 km	1 MPa/km	
Thermal anomalies		
Alpine Fault, New Zealand	100 MPa	Scholz (1980)
San Andreas Fault, Calif.	< 25 MPa	Lachenbruch and Sass (1973), Turcotte et al. (1980)
Stress drops		
San Andreas Fault, Calif.	< 10 MPa	Raleigh and Evernden (1981)
Models of intraplate stresses	10–15 MPa	Solomon et al. (1980)
Conversion of convective heat to mechanical work	10–20 MPa	McKenzie and Jarvis (1980)
Mass-excess loading-compensation	> 50 MPa	McNutt (1980), Lambeck (1980)

static friction on a surface with a normal stress $\bar{\sigma}_n$ across it (Brace and Kohlstedt, 1980; Kirby, 1983). The stress required for slip may be reduced by a reduction of $\bar{\sigma}_n$ in eqn. (2) by pore fluid pressure as shown experimentally (e.g., Handin et al., 1963). This concept is consistent with the triggering of the Denver (Healy et al., 1968) and Rangely earthquakes (Raleigh et al., 1972; Handin and Raleigh, 1972; Raleigh, 1977).

More recently Haimson and Doe (1983) have challenged the universalality of Byerlee's relation and McGarr's data. Their 13 hydrofracturing tests of Illinois Precambrian granite at depths 686 to 1449 m give

$$\tau_m = 9.4 + z \qquad (3)$$

The relations (1) and (3) predict similar shear stresses at 800 m but at say 5 km, eqn. (1) predicts a stress of 38 MPa as compared with 14.4 MPa from eqn. (3), a difference which becomes larger with extrapolation to greater depths. T. Engelder (pers. commun., 1986) has compiled complete data sets for three other localities and all fall near the results obtained by Haimson and Doe (1983). Finally, Zoback and Mastin (1986) calculated a maximum breakout stress of 150 MPa at 11.6 km in the Kola wellbore, a value appreciably lower than that predicted by Byerlee's relation.

Arguments based on extrapolations to normal stresses at depths greater than about 5 km of laboratory rock friction data lead to high deviatoric stresses, but these arguments are of questionable validity. A similar situation, recognized by Kirby (1980) and others, occurs in extrapolations of high temperature creep flow laws to lower temperature–pressure environments, where other processes may dominate the creep strain and thus govern different functional relationships. Such extrapolations, to physical conditions beyond their range of validity, lead to overestimates of stress differences; this topic forms part of the basis of this paper and will be discussed more fully subsequently.

Certain microstructures induced by dominantly ductile deformations, properly calibrated by laboratory experiments, depend to first order, only on deviatoric stress and thus show great promise as indicators of stress levels at depth (Table 3). Mechanical twins in calcite, dolomite and clinopyroxene develop at critical resolved shear stresses of 10, 100 and 140 MPa, respectively (Tullis, 1980). More extensively applied microstructures, dependent only on *steady-state* deviatoric stress, are free dislocation densities, subgrain (polygonized) diameters and recrystallized grainsize. These paleopiezometers are also relatively easy to apply but must not be used indiscriminately; they are undergoing continuing refinement. Twiss (1986) has provided a theoretical discussion of dislocation density and subgrain size as applied primarily to quartz and olivine. Kohlstedt and Weathers (1980) summarize applications by several workers of all

three techniques to deformed quartz in several major fault zones, the shearing stresses so determined ranging from 10 to 100 MPa (Table 3). Similar stress values were observed in quartz deformed during folding of the Marquette Synclinorium, Michigan (Kappmeyer and Wiltschko, 1984). These techniques have been established for calcite (Schmid et al., 1980; Friedman and Higgs, 1981) and have been applied to limestones from the Helvetic zone of the Swiss Alps (Pfiffner, 1982). All three paleopiezometers are available for olivine (e.g., Post, 1973; Kohlstedt et al., 1976; Ross et al., 1980; Karato et al., 1980) but only subgrain size and recrystallized grainsize has been applied extensively to upper mantle materials (e.g., Mercier et al., 1977; Mercier, 1980b; Avé Lallemant et al., 1980; Nicolas et al., 1980).

Other estimates of deviatoric stress in the continental lithosphere have been based primarily on: (1) thermal anomalies adjacent to fault zones; (2) seismic-energy radiation; (3) forces associated with plate tectonic models; and (4) strengths required to support surface loads and gravity anomalies. The high thermal anomalies along several major fault zones, such as the Alpine Fault, New Zealand, may be associated with shear heating at stresses near 100 MPa at rates of slip compatible with reasonably well-established plate velocities, but localized high rates of displacement along the faults could lower the shear stresses required appreciably (Scholz, 1980). Because of the absence of any significant heat flow anomaly, the average shear stress along the San Andreas fault zone to a depth of 20 km appears to be at most a few tens of MPa (Lachenbruch and Sass, 1973). Leary (1985) reached the same conclusion based on nearsurface stress and displacement measurements incorporated into a two-layer elastic model. Indeed, Raleigh and Evernden (1981) have suggested that the < 10 MPa stress drop typically inferred from seismic-energy radiation from plate-boundary faults may represent the total stress drop rather than a lower limit as is generally supposed.

On the other hand, Sibson (1982) has argued for shearing resistances near 50 MPa in the top 12 km of parts of the San Andreas, based on Byerlee's (1978) relation, the wet quartzite flow law of Koch et al. (1980) and strain rates of 10^{-11} to 10^{-12} s^{-1} over a 1 km wide zone. In a subsequent analysis (Sibson, 1984), the flow laws for wet granite and diorite of Hansen and Carter (1982), in conjunction with the other arguments, were used to estimate the depth-dependence of frictional resistance and transition from frictional to semi-brittle behavior. For the San Andreas, and strike-slip faults in general, Sibson estimates the peak shear resistance, corresponding to the brittle–smi-brittle transition, to be about 100 MPa at about 13 km for quartz-bearing rocks and about 150 MPa at 18 km for feldspathic rocks, assuming a strain rate of near 10^{-11} s^{-1}, a thermal gradient of 25°C/km and a hydrostatic pore pressure. However, these analyses ignore anomalous fluid pressures, pressure solution, and clay minerals (Sibson, 1982, 1984) all of which may occur and would lower the shear resistance significantly. A somewhat similar argument has been used by Meissner and Strehlau (1982), employing the wet quartzite flow law of Parrish et al. (1976), to show that maximum earthquake frequencies of many faults, in the depth range 5 to 10 km, correspond approximately with predicted peak stress values averaging near 150 MPa for a wet upper crust only.

On the still larger scale, plate-tectonic models of interplate stresses and of orientations of midplate principal stresses provide constraints on the magnitude of deviatoric stresses in the lithosphere (Solomon et al., 1980). Shear stresses at plate boundaries are approximately the same as in plate interiors, about 10 to 15 MPa. Mean shearing stresses at plate boundaries of 10 to 20 MPa result from estimates of the efficiency with which convection can convert heat into mechanical work (McKenzie and Jarvis, 1980). However, because of large negative buoyancy forces associated with subducting slabs that do not penetrate a depth of 650 km, frictional resistances near 200 MPa are required to balance these forces unless mantle viscosities are at least 5×10^{22} poises (Davies, 1980). Viscosities of this magnitude, and higher, are calculated here for strain rates in the range 10^{-15}–10^{-17} s^{-1} for both continental and oceanic geotherms in the depth range 100–400 km.

For oceanic regions, estimates of shearing stresses (ca. 50 MPa) required to support long-term loads, based on gravity, topography, isostatic and

rock mechanics observations, are relatively straight forward (e.g., McNutt, 1980; Watts et al., 1980; McNutt and Menard, 1982; Kirby, 1983). While similar values of stress, maintained over timespans near 100 Ma, are estimated for certain continental regions (McNutt, 1980; Lambeck, 1980), the problem is much more complicated, again because of large differences in tectonic environment, reflecting differences in geological and geophysical processes (McNutt, 1980, 1983; Forsythe, 1985; McNutt and Kogan, 1987; Kogan and McNutt, 1987). Depending on thermal regime and other factors, the compensation ranges from regional to very local and the maximum effective elastic thickness (high flexural rigidity) increases with age from the time of loading, consistent with thermally-activated creep relaxation. However, Forsythe (1985) shows that flexural rigidities, commonly estimated from surface loading of a laterally homogeneous elastic plate, are appreciably lower than those obtained if internal and subsurface buoyant loading are taken into account. Subsurface loading results in continental regions from common dynamic processes such as intrusions and diapirism, metamorphism and phase changes, large-scale mass transport by ductile faulting, subduction, and other mechanisms and by heating and cooling of the lithosphere in general. Analyses including both surface and subsurface loading lead to effective elastic plate thicknesses of a few tens of kilometers as opposed to a few kilometers.

In summary, shear stresses in the continental lithosphere measured to 5 km or inferred from several indirect methods appear to range from 1 to 150 MPa. As we shall show below, shear stresses obtained by extrapolation of empirically-determined steady-state flow laws fall within this rather broad range.

Flow properties of continental crustal crystalline rocks

It is generally recognized, both from geological studies and from laboratory investigations, that most crystalline rocks deform predominantly by brittle mechanisms in the uppermost part of the crust, through semi-brittle and grain boundary mechanisms at upper-mid-crustal depths, to ductile mechanisms deep in the crust. Depth range in which these transitions occur vary widely, depending critically on rock constitution, temperature gradient, effective pressure, chemical environment and on the state of stress. Techniques, capabilities and limitations of experimental studies of rock deformation to date are presented in a comprehensive review by Tullis and Tullis (1986), and the mechanical response compiled for a wide variety of rock types are tabulated by Kirby (1983) and Kirby and McCormick (1984).

Rutter (1986) has recently addressed nomenclature problems, arriving at virtually the same nomenclature as Griggs and Handin (1960). He focuses on the misuse of the term ductile and on transitions between regimes, such as the commonly used brittle–ductile transition interpreted for seismic–aseismic transitions, as brittle–plastic transitions. We are in general agreement with his conclusions that the term ductile should be restricted to macroscopic homogeneous deformations though, from common usage in microdynamics, ductile mechanisms generally imply normal-stress independent mechanisms such as dislocation processes. We are concerned here more with the "brittle–ductile" (microplasticity) transition, which we refer to as the semi-brittle regime (Carter and Kirby, 1978) and which is likely to dominate at midrange depths of the continental crystalline crust.

Brittle field

Paterson (1978), Brace and Kohlstedt (1980) and Kirby (1980, 1983, 1985) have recently summarized the major strength properties of rocks deforming in the brittle field. The fracture strength of rocks increases markedly with pressure but varies widely with rock type (Brace and Kohlstedt, 1980). While the effects of temperature and strain rate are relatively small, fracturing is clearly thermally-activated (e.g., Friedman et al., 1979; Kranz, 1983; Atkinson, 1984) presumably through stress-aided chemical corrosive processes and mobilization of dislocations at tips of microcracks that grow and coalesce to form macroscopic fractures.

At a given pressure, then, the fracture strength should depend on the properties, distribution and densities of individual cracks and on stress concentrations as well as the thermal and chemical environment. However, there is no acceptable theory which adequately predicts fracture strength under general compressive or tensile states of stress. A lower bound is placed by the constraint that the stress difference required can not fall below that necessary for frictional sliding along existing faults oriented optimally for sliding (Kirby, 1983).

Byerlee's (1968) relation (eqn. 2) is based primarily on observations of frictional resistance of rock–rock surfaces. Simulated fault gouges of anhydrous silicates, carbonates, sulfides, sulfates and phosphates also appear to follow Byerlee's law fairly closely (Shimamoto and Logan, 1981). However, weaker materials in gouge zones, such as halite, clay minerals and chlorite, lower the fault strength (e.g., Wang et al., 1980; Friedman et al., 1984; Shimamoto, 1985b). However, if clays are dehydrated by increasing the temperature, the fault strength may increase and the mode of sliding may change (Logan et al., 1981). This, then, raises a question concerning the nature of permeability in fault gouge during natural deformations (Etheridge et al., 1984; Kerrich et al., 1984; Morrow et al., 1984; Dula, 1985; Raleigh and Marone, 1986).

The time-dependence of friction gives rise to stick-slip behavior, precursive slip, and creep at constant normal and shearing stress (Kirby, 1983). Shimamoto and Logan (1986) have observed a marked change in the mode of slip as well as friction coefficient (which increased from about 0.38 to 0.47) in halite gouge deformed at shearing strain rates decreasing by about five orders of magnitude. Dieterich and Conrad (1984) have shown that dry surfaces of Eureka quartzite consistently yield a coefficient of friction between 0.85 and 1.0 as compared with 0.55 to 0.65 for the tests in a humid environment. They suggest that water may reduce the surface indentation hardness of gouge or may promote plasticity within gouge grains; in any instance, reduction of gouge grain size during sliding indicates that microfracturing is promoted by moisture. They also conclude that an overall diminution of frictional strength accompanies increases in displacement and velocity; this generality may not hold, however, if plasticity increases the real contact area of asperities. Weeks and Tullis (1985) have demonstrated some different trends for frictional sliding of dolomite marble; steady-state velocity strengthening occurs, frictional strength decays with velocity, and friction parameters vary strongly with velocity, perhaps being more strongly time- rather than displacement-dependent.

It is clear from the few observations given above that rock frictional resistance is a very complex physical phenomenon requiring additional research investigating geologically reasonable physical–chemical environmental conditions and materials and their time, temperature, velocity and displacement dependencies, as well as stress and/or strain histories (Olsson, 1984; Chester, 1985; Logan and Feucht, 1985). For these reasons, we believe that frictional resistance along natural faults is likely to decrease nonlinearly with depth and that Byerlee's relation represents an upper bound that is useful only near the Earth's surface. If these perceptions are correct, they call into question some of the results of recent extensive analyses and interpretations of mechanics of fold-and-thrust belts and accretionary wedges based on the Coulomb criterion (Davis et al., 1983; Dahlen, 1984; Dahlen et al., 1984).

The expected deviation from Byerlee's relation at about 5 km depth is emphasized here because many yield surfaces of the type first presented for olivine by Goetze and Evans (1979) and shown in Fig. 2A have appeared in the literature, to this date, in support of arguments for high stress levels associated with various deformational processes. These published yield surfaces begin with the assumption that the friction relation may be extrapolated linearly to depths below 10 km until it intersects a stress–depth profile for steady-state flow of some selected material, whereupon the flow stress diminishes with depth. The depth of intersection, and hence peak stress difference, depends on the creep flow law selected for the problem which itself may be extrapolated out of its range of validity. Kirby (1983) has modified the original yield surface (Fig. 2B) by introducing

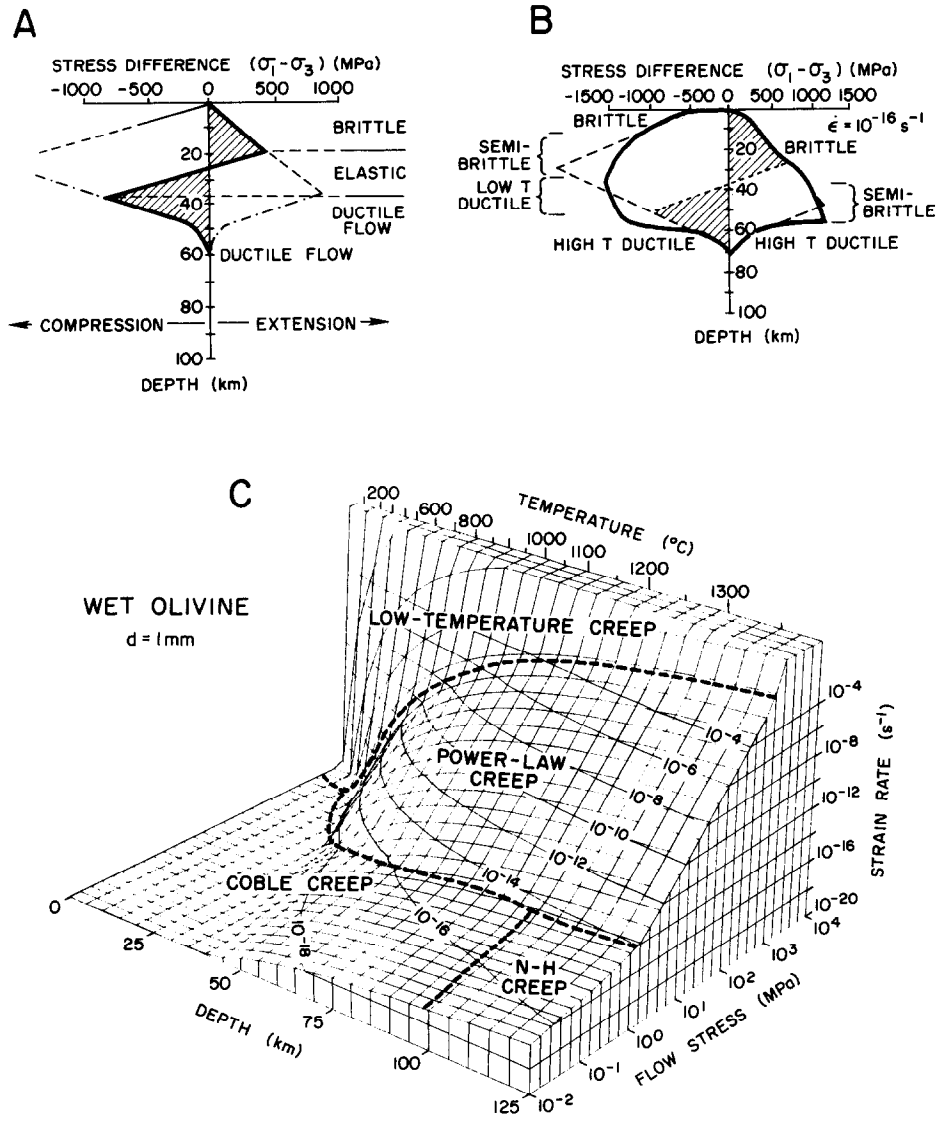

Fig. 2. A, B. Yield envelopes and stress profiles for olivine involved in plate bending; ruled area shows the bending moment given by integrated bending stresses. (A) is the original envelope of Goetze and Evans (1979) and (B) is that modified for estimated regions of low temperature ductile and semi-brittle flow at a strain rate of 10^{-16} s^{-1} (Kirby, 1983). C. Deformation surface showing flow regimes and processes for peridotites and dunite (Tsenn and Carter, 1987).

estimated semi-brittle and low-temperature ductile fields for olivine in his analysis of flexure of the oceanic lithosphere.

For faults in continental crust, the linear rock–friction relation representation is in apparent conflict with gradual changes with depth of the general nature and processes within fault zones proposed by Sibson (1983, fig. 2). In this slightly modified scheme: (1) gouge is produced by water-enhanced brittle behavior to about 5 km; (2) cataclasis, semi-brittle, and grain boundary solution and diffusion processes (cataclasites) occur to about 10 km; (3) cataclasites then grade into mylonites dominated by combinations of grain boundary processes and dislocation creep, including dynamic recrystallization (Sakai and Jonas, 1984; Urai et al., 1986). Recent discussions of semi-brittle and ductile faulting bear on regimes (2) and (3) and will be discussed below. Sibson's general perceptions and observations are con-

sistent with earthquake frequency distribution in the depth range 2–15 km (e.g., Meissner and Strehlau, 1982) where brittle, semi-brittle, grain boundary and dislocation creep processes all contribute to the deformational state and strength.

If this progression even reasonably approximates actual processes occurring along fault zones at depth, then yield envelopes representative of the depth-dependent strength will need to be developed by means of experiments carefully designed to simulate geological conditions much more closely. In addition to keen perceptions and current observations, experimental work must be guided and verified by drilling through active fault zones at various depths.

Semi-brittle field

For crystalline rocks at moderate crustal depths dislocation glide, dislocation and diffusion creep and other highly thermally activated processes begin to operate at the crystal scale and the rocks begin to flow in the semi-brittle regime. In this transitional regime, dislocation processes may

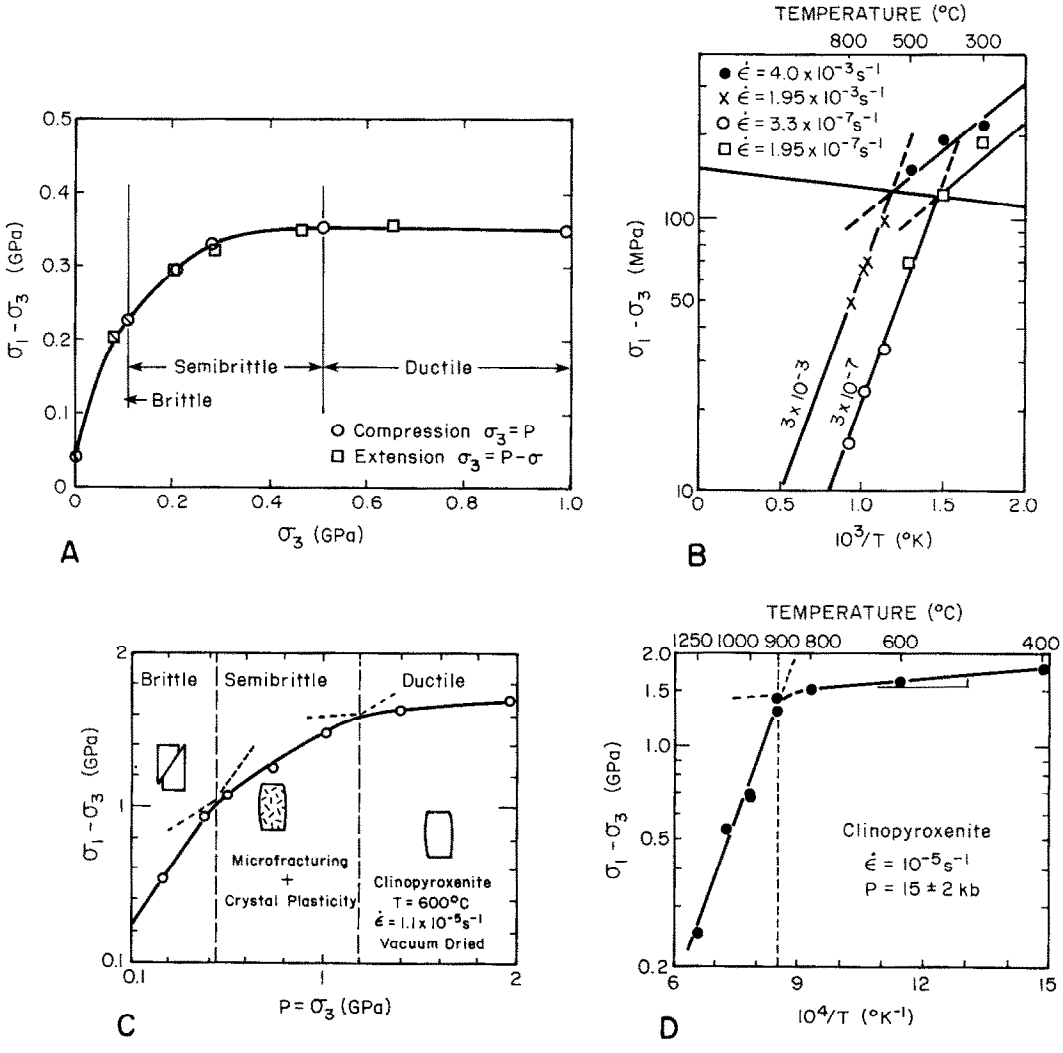

Fig. 3. A, C. Diagram showing brittle, semi-brittle and ductile regimes at constant temperature and strain rates for marble (A) and clinopyroxenite (C—modified after Kirby, 1980). B. Breakdown from high-temperature to low-temperature ductile creep for marble (B) and clinopyroxenite (D—modified after Kirby, 1980; Kirby and Kronenberg, 1984).

serve to retard or aid fracturing so that both ductile and brittle mechanisms contribute to the creep strain. Carter and Kirby (1978) pointed out that such behavior, and largely ignored transient creep, might be most important for crustal deformation of crystalline rocks over a wider range of depth. Kirby (1980) has elaborated on this concept and has shown that it applies to monomineralic aggregates of relatively soft minerals, such as calcite, as well as to hard ones, such as clinopyroxene. Figure 3A shows typical data for Yule marble compiled by Kirby from Handin (1966) and Fig. 3C shows similar data for Sleaford Bay clinopyroxenite (Kirby, 1980; Kirby and Kronenberg, 1984). For both materials, the differential stress represents either the ultimate strength or the stress at 5% (marble) or 10% (clinopyroxenite) strain plotted against σ_3. Note that for both materials (Figs. 3A, C) extrapolation of data from any regime into another, that is, out of their range of validity, would lead to *serious overestimates* of the flow stress.

Increasing the confining pressure in the semi-brittle regime does increase the strength and the post-yield slope of stress–strain curves as shown for Carrara marble by Von Karman (1911) and, more recently, by Kirby (1980); minerals that show some plasticity at room temperature can be rendered ductile simply by raising the confining pressure. For stronger materials, such as silicates, an increase in temperature at pressure and a decrease in the rate of strain has a similar effect. Steady-state flow can be achieved for both types of materials deforming in the semi-brittle regime. The pressure, temperature or strain-rate increment required depends critically on the water content and partial pressure of H_2O.

Weakening effects other than the purely mechanical effect of pore pressure so important in the brittle field occur in the semi-brittle and ductile regimes. These chemical effects of H_2O involve hydrolytic weakening including pressure-enhanced diffusivity or solubility of water into silicate grains, pressure solution, bulk solid and grain boundary diffusion and promotion of dislocation creep, recovery and recrystallization. These various weakening and ductility-enhancing effects, which require only trace amounts of water in some materials, occur during deformation and metamorphism and are accompanied by modifications of defect chemistry. They have been discussed extensively recently by e.g., Blacic (1975, 1981); Tullis (1979); Tullis et al. (1979); Yund and Tullis (1980); Kirby (1980, 1984); Hobbs (1981, 1983, 1984); Rutter (1983); Blacic and Christie (1984); Green (1984); Mainprice and Paterson (1984); Jaoul et al. (1984); Kronenberg and Tullis (1984); Etheridge et al. (1984); Giletti and Yund (1984); Aines et al. (1984); Brodie and Rutter (1985); Mackwell et al. (1985); Ord and Hobbs (1986); Boland and Tullis (1986); Freund and Oberheuser (1986); Paterson (1986); Rovetta et al. (1986); and Kronenberg et al. (1986). Kronenberg et al. (1986) have shown that diffusion of molecular water into the quartz crystal structure is required for hydrolytic weakening and that diffusivity is too slow to account for such weakening in laboratory times. They suggest that the observed weakening results from penetration of water along microcracks and other flaws in the crystal allowing local weakening and plastic flow. Measurements and interpretations of Rovetta et al. (1986) and of Kronenberg et al. (1986) are in close accord.

Composite polycrystalline aggregates, most representative of crustal rocks, generally exhibit bulk semi-brittle behavior over a larger depth range than monomineralic aggregates because certain mineral species may be ductile under the same conditions that other phases are brittle. Thus, Tullis and Yund (1977) observed in experiments on dry Westerly granite at a strain rate of 10^{-6} s^{-1} that at pressures above 500 MPa the transition from dominant microfracturing to dominant dislocation motion occurred over the temperature ranges 300° to 400°C for quartz and 550° to 650°C for feldspar. These temperature ranges were reduced by about 150°–200°C in subsequent experiments conducted at 1.5 GPa pressure with the addition of 0.2 wt.% distilled water and yield stresses are significantly lower (Tullis and Yund, 1980). For the granite, Enfield aplite and Hale albite, a pressure-dependent critical temperature exists (900°C for feldspars and 750°C for quartz) above which hydrolytic weakening takes place; increasing pressure from 500 to 1500 MPa increases the solubility or equilibrium water con-

centration in the crystal structure (Tullis et al., 1979). Gandais and Willaime (1984) report somewhat similar behavior of feldspar single crystals and suggest that at natural strain rates, at 0.2 to 1.0 GPa pressure, feldspars behave plastically above 500 °C.

Carter et al. (1981) and Hansen and Carter (1983) carried out constant stress experiments on Westerly granite at 1.0 GPa pressure, entirely within the α-quartz stability field (470 ° to 765 °C). The weakening effects of the additional 0.1 wt.% H_2O were most pronounced in experiments at the lower creep stresses and attendant strain rates. Most of these experiments were carried out to low strains ($< 10\%$) and it was suggested from analyses of the specimens and arguments concerning values of creep activation energies that ductile flow of quartz (ca. 27 vol.%) controlled the creep rates. This suggestion was confirmed by Ross et al. (1983) and it also appears to hold for many naturally deformed granitic rocks deformed to low strains (Carter et al., 1981). For those deformed to higher strains, such as granitic rocks associated with shear zones and highly deformed crystalline nappe complexes (e.g., Hanmer, 1982; Gandais and Willaime, 1984), semi-brittle and ductile deformation of the feldspars become important as in the relatively high (ca. 20%) strain experiments of Tullis and Yund. In any instance, granites deformed under most experimental and natural conditions examined to date deform predominantly in the semi-brittle regime (e.g., Carter et al., 1981; Lespinasse and Pecher, 1986).

The foregoing generalization also appears to apply to experimentally and naturally deformed polymineralic rocks of intermediate to mafic composition (e.g. Kronenberg and Shelton, 1980; Caristan 1980, 1982; Hansen, 1982; Brodie and Rutter, 1985, 1987). Kronenberg and Shelton (1980) studied the flow mechanisms in pyroxene and plagioclase of Maryland diabase (58% px., 36% plag.) deformed dry at 0.5 to 1.5 GPa pressure, temperatures from 600 ° to 1000 °C and strain rates of 10^{-4} to 10^{-6} s^{-1}. Both phases deform by microfracturing, mechanical twinning and intracrystalline slip. The relative importance of each process, respectively, increases with increasing pressure, temperature and decreasing strain rate. At a strain rate of 3×10^{-6} s^{-1} at temperatures > 800 °C, plagioclase is the more highly deformed phase with much higher dislocation density whereas at lower temperature, both phases deform approximately equally. However, Caristan (1980, 1982), who used several loading paths in deforming Maryland diabase (47% px., 49% plag.) at pressures to 450 MPa and temperatures to 1000 °C concluded that at 1000 °C, plagioclase and pyroxene contribute approximately equally to the creep strain. With increasing pressure, Caristan (1982) observed three generally temperature- and strain rate-sensitive domains: (1) a positive pressure-sensitive domain (strain rate insensitive) corresponding to brittle behavior; (2) a negative pressure-sensitive domain characterized by transitional (semi-brittle) behavior; and (3) the pressure-insensitive domain dominated by dislocation creep.

The brittle–ductile transition boundary determined by Kronenberg and Shelton (1980), though determined at different physical conditions, lies near the transitional field of Caristan and the flow laws obtained are similar (Shelton and Tullis, 1981; Caristan, 1982). Kronenberg and Shelton (1980), who performed comparable experiments on Sleaford Bay clinopyroxenite and Adirondack anorthosite, observed that deformation microstructures compared closely with those observed in each major phase of the diabase and considered the possibility of summing creep strain rates according to volume fractions and flow laws for each phase. They concluded, however, because of the ophitic texture of the diabase, with plagioclase providing a stress-supporting framework, that deviatoric stresses imposed on the two phases are not equivalent, precluding a simple summation.

Hansen (1982) carried out a series of constant stress experiments at 1.0 GPa confining pressure and temperatures from 768 ° to 1150 °C on wet quartz (6%) diorite (65% plag., 27% px.). Pyroxenes are either undeformed or show mild undulatory extinction while quartz grains are highly deformed by plastic deformation and show subgrain formation and recrystallization. Feldspars are extensively deformed by pervasive extension fractures, sharp undulatory extinction, subgrain formation, grain boundary recrystallization and

transgranular fault zones containing cataclastic gouge. Therefore the overall deformation of the wet specimens is semi-brittle and Hansen concludes that deformation of feldspars exerts primary control over the creep rate.

Ductile field

Rock flow properties and processes in the ductile regime, and their dependencies on the several physical/chemical variables have also been summarized recently (e.g., Heard, 1976; Carter, 1976; Nicolas and Poirier, 1976; Tullis, 1979; Handin and Carter, 1980; Kirby, 1980, 1983, 1985; Kirby and McCormick, 1984; Poirier, 1985) and need not be repeated here. In general, the ductile field is characterized by a very small pressure effect on strength ($d\sigma/dP < 0.1$), a lack of pressure effect on hardening rate, abundant evidence for dislocation and diffusion-assisted mechanisms and no significant dilatancy. Many of these characteristics also apply approximately near the ductile boundary within the semi-brittle regime (Fig. 3).

Low-temperature ductile field

In the low-temperature ductile regime where flow is decelerating (transient) or work-hardening, strength is relatively insensitive to strain rate and temperature; this is illustrated for Yule Marble (Fig. 3B) and for Sleaford Bay clinopyroxenite (Fig. 3D). The strain rate and temperature dependencies of flow strength are much higher in the high temperature ductile regime (Figs. 3B and 3D; left) in accord with extensive experience with metals (Weertman and Weertman, 1975, 1983). Similar behavior is well-documented for synthetic (Heard, 1972) and natural (Handin et al., 1986) halite and less well so for orthopyroxenite (Raleigh et al., 1971) and dunite (Kirby, 1980). The change in flow properties from low to high temperatures in the ductile regime corresponds to a change in rate-controlling deformation mechanisms, generally from restricted dislocation glide (slip, twinning) to dislocation creep (including glide, climb and cross-slip) and other mechanisms in which diffusion is operative and commonly rate-limiting. Notice, once again, this most important point: invalid extrapolations of data into either regime leads to very significant overestimates of the flow stress (Figs. 3B and 3D).

Kirby (1980, p. 6356) states that there is a clear strain rate dependence of the transition temperature (fig. 1b and fig. 9 of Kirby, 1980). While there may be a strain-rate dependence, Tsenn and Carter (1987) show that this dependence is weak. They explore four methods for estimating the stress at the transition from high temperature to low temperature ductile creep (commonly referred to as power law breakdown, PLB and breakdown stress, σ_b) and conclude, that $\sigma_b \cong 10^{-2}\,\mu$ (where μ is the shear modulus), provides the most satisfactory estimate for silicates. Thus PLB or σ_b occurs at very high stresses as shown, for example, on the olivine deformation surface of Fig. 2C. Such high stresses, if ever attained in natural deformations, might generally occur at low temperatures and hence low pressures where low-temperature ductile creep may compete with semi-brittle or brittle mechanisms and may therefore be suppressed entirely.

High-temperature ductile field

The materials selected for this analysis and their steady-state flow parameters are listed in Table 4; Kirby (1983), Kirby and McCormick (1984) have given a more nearly complete documentation of flow laws available to 1984. In general: (1) results obtained from liquid and gas confining medium apparatus are regarded as most reliable; (2) dry tests in a rocksalt confining medium in solid pressure medium equipment are next most reliable; (3) most wet tests in solid pressure medium apparatus are regarded as less reliable (because the partial pressure of water is unknown and may vary with time); and (4) results from assemblies using AlSiMag are least reliable. Materials with average grain diameters appreciably larger than 0.1 sample cylinder diameter, such as the anorthosite data of Shelton and Tullis (1981) have also been omitted from consideration as it has been shown that relatively large grain diameter/sample diameter ratios yield unreliable mechanical data. Of the several load paths used, results from stress relaxation tests are largely ignored because they are not yet well-understood; however, these tests, which generally yield lower

TABLE 4

Steady-state flow properties and processes: $\dot{\epsilon} = A \exp(-Q_c/RT)\sigma^n$

Material, source	Confining pressure, medium	Test type, condition compression [1]	Published flow parameters [2] Q_c in kJ/mole, $A = \text{MPa}^{-n}\text{s}^{-1}$	Refit parameters [4]	Flow mechanisms
Polycrystalline Galena (Atkinson, 1976)	150 MPa fluid	constant strain rate $T = 300° - 400°$ C $\dot{\epsilon} = 3.1\times10^{-4} \sim 3.4\times10^{-8}$ s^{-1} $\Delta\sigma = 33$–110 MPa	log $A = -11.1$ $Q_c = 94 \pm 15$ $n = 7.3 \pm 0.6$		subgrain formation, dislocation creep
Avery Island Rocksalt (Hansen and Carter, 1984)	3.5–21 MPa fluid	creep tests $T = 100° - 200°$ C $\dot{\epsilon} = 1.7\times10^{-6} - 1.3\times10^{-9}$ s^{-1} $\Delta\sigma = 1.5$–20.7 MPa	log $A = -3.1$ $Q_c = 66.5 \pm 8.7$ $n = 4.5 \pm 0.6$		subgrain formation, dislocation creep
Polycrystalline Anhydrite (Müller and Briegel, 1978)	150 MPa fluid	constant strain rate, stress relaxation $T = 350° - 450°$ C $\dot{\epsilon} = 10^{-5} - 7\times10^{-7}$ s^{-1} $\Delta\sigma = 50$–212 MPa	log $A = 1.5$ $Q_c = 152.3 \pm 9.4$ $n = 2$		dislocation glide, twinning, possible grain boundary sliding
Yule Marble 1 cylinder (Heard and Raleigh, 1972)	500 MPa gas extension	constant strain rate $T = 500° - 800°$ C $\dot{\epsilon} = 2\times10^{-3} - 3.3\times10^{-8}$ s^{-1} $\Delta\sigma = 15$–110 MPa	log $A = -3.9$ $Q_c = 259.3 \pm 12.2$ $n = 8.3 \pm 0.4$		dislocation glide, subgrain formation, grain boundary recrystallization
Carrara Marble regime 2 (Schmid et al., 1980)	300 MPa gas	constant strain rate $T = 700° - 1000°$ C $\dot{\epsilon} = 6.7\times10^{-3} - 5.3\times10^{-6}$ s^{-1} $\Delta\sigma = 24$–93 MPa	log $A = 3.1$ $Q_c = 418 \pm 84$ $n = 7.6 \pm 1.6$		extensive subgrain formation; grain boundary migration; possible sliding
Solenhofen limestone regime 3 (Schmid et al., 1977)	300 MPa gas	constant strain rate $T = 600° - 900°$ C $\dot{\epsilon} = 7.9\times10^{-4} - 7.3\times10^{-7}$ s^{-1} $\Delta\sigma = 1$–99 MPa	log $A = 4.3$ $Q_c = 213 \pm 16$ $n = 1.7 \pm 0.2$		grain boundary sliding, slip, recrystallization
Simpson quartzite Dry (Koch, 1983)	1100 MPa copper	constant strain rate $T = 800° - 900°$ C $\dot{\epsilon} = 2.0\times10^{-4} - 1.4\times10^{-7}$ s^{-1} $\Delta\sigma = 139$–2912 MPa	log A $= -6.9$ $Q_c = 134 \pm 64$ $n = 2.72 \pm 0.4$		dislocation glide, dislocation creep, grain boundary recrystallization
Quadrant quartzite Wet (0.03 wt.% H_2O added) (Hansen, 1982)	1000 MPa talc (α-quartz field)	creep tests $T = 660° - 760°$ C $\dot{\epsilon} = 1.3\times10^{-5} - 4.7\times10^{-7}$ s^{-1} $\Delta\sigma = 400$–920 MPa	log A $= -1.5$ $Q_c = 172.6$ $n = 1.9$		dislocation glide, dislocation creep, grain boundary migration

Westerly granite Dry (Hansen and Carter, 1983)	1000 MPa talc (α-quartz field)	creep tests $T = 640° - 770°$ C $\dot{\epsilon} = 1.1 \times 10^{-5} - 1.2 \times 10^{-7}$ s^{-1} $\Delta\sigma = 510-1260$ MPa	log A = −5.7 $Q_c = 186.5$ $n = 3.3$		semibrittle behavior, ductile mechanisms increase in abundance with increasing temperature dislocation glide, some dislocation creep in quartz, microfracturing
Westerly granite Wet (0.1 wt.% H_2O added) (Hansen and Carter, 1983)	1000 MPa talc (α-quartz field)	creep tests $T = 546° - 760°$ C $\dot{\epsilon} = 1.5 \times 10^{-5} - 10^{-7}$ s^{-1} $\Delta\sigma = 360-1205$ MPa	log $A = -3.7$ $Q_c = 140.6$ $n = 1.9$		semibrittle behavior, enhanced ductility over dry counterparts dislocation glide, dislocation creep in quartz, microfracturing
Enfield aplite Dry (Shelton, 1981; Shelton and Tullis, 1981)	1500 MPa NaCl	creep tests T, σ-incremental $T = 700° - 900°$ C $\dot{\epsilon} = 1.7 \times 10^{-5} - 10^{-7}$ s^{-1} $\Delta\sigma = 170-600$ MPa	log $A = -6.6$ $Q_c = 163.2$ $n = 3.1$	log $A = -5.2$ $Q_c = 193 \pm 46$ $n = 3.1 \pm 0.8$ $r = 0.92$	homogeneous strain, mechanisms not described
Hale albite rock Dry (Shelton, 1981; Shelton and Tullis, 1981; Shelton et al., 1981)	1500 MPa NaCl and $CaCO_3$	creep tests T, σ-incremental $T = 725° - 1100°$ C $\dot{\epsilon} = 1.7 \times 10^{-5}, 4.3 \times 10^{-8}$ s^{-1} $\Delta\sigma = 150-940$ MPa	log $A = -5.63$ $Q_c = 234.2$ $n = 3.9$	log $A = -2.3$ $Q_c = 245 \pm 22$ $n = 2.8 \pm 0.4$ $r = 0.98$	dislocation glide, dislocation creep
Orthopyroxenite Dry (Raleigh et al., 1971)	500–2000 MPa gas and talc AlSiMag	constant strain rate stress relaxation T-incremental $T = 840° - 1100°$ C $\dot{\epsilon} = 10^{-4} - 10^{-7}$ s^{-1} $\Delta\sigma = 100-400$ MPa	log $A = -0.5$ $Q_c = 293$ $n = 2.4$		dislocation glide, dislocation creep
Orthopyroxenite Wet (Talc dehydration) (Ross and Nielsen, 1978)	1000 MPa talc	constant strain rate stress relaxation, T-incremental $T = 950° - 1300°$ C $\dot{\epsilon} = 10^{-4} - 10^{-7}$ s^{-1} $\Delta\sigma = 160-1050$ MPa	log $A = -2.2$ $Q_c = 271 \pm 18$ $n = 2.8 \pm 0.5$		dislocation glide, dislocation creep, dynamic recrystallization

TABLE 4 (continued)

Material, source	Confining, pressure, medium	Test type, condition compression [1]	Published flow parameters [2] Q_c in kJ/mole, $A = MPa^{-n}s^{-1}$	Refit parameters [4]	Flow mechanisms
Websterite (68% CPX, 32% OPX) Dry Avé Lallemant, 1978)	1000 MPa talc + AlSiMag	constant strain rate, T, $\dot{\epsilon}$-incremental $T = 1000° - 1200°C$ $\dot{\epsilon} = 2 \times 10^{-5} - 10^{-7}\ s^{-1}$ $\Delta\sigma = 300-700$ MPa	$\log A = -6.4$ $Q_c = 326 \pm 38$ $n = 4.3 \pm 1.2$	$\log A = 5.5$ $Q_c = 323 \pm 65$ $n = 4.3 \pm 1.3$ $r = 0.93$	dislocation glide, dislocation creep, dynamic recrystallization
Clinopyroxenite Dry (Kirby and Kronenberg, 1984)	1500 MPa NaCl or NaF	constant strain rate $T = 800° - 1100°C$ $\dot{\epsilon} = 10^{-4} - 10^{-7}\ s^{-1}$ $\Delta\sigma = 480-1140$ MPa	$\log A = -5$ $Q_c = 380$ $n = 5.3$	$\log A = -7.8$ $Q_c = 330 \pm 84$ $n = 5.8 \pm 1.8$ $r = 0.97$	multiple slip, dislocation creep, dynamic recovery
Clinopyroxenite Wet (0.5–1.0% H_2O added) (Boland and Tullis, 1986)	360 MPa gas	constant strain rate T-incremental stress relaxation $T = 990° - 1271°C$ $\dot{\epsilon} = \sim 10^{-5} - 10^{-6}\ s^{-1}$ $\Delta\sigma = 79-249$ MPa	$\log A = 5.17$ $Q_c = 490 \pm 159$ $n = 3.3 \pm 0.9$		dislocation glide, twins, dislocation creep, grain boundary migration
Maryland Diabase Dry (Caristan, 1980, 1982)	450 MPa gas	creep tests σ-incremental $T = 900° - 1000°C$ $\dot{\epsilon} = 1.5 \times 10^{-5} - 1.7 \times 10^{-7}\ s^{-1}$ $\Delta\sigma = 90-296$ MPa	$\log A = -1.2$ $Q_c = 276 \pm 14$ $n = 3.05 \pm 0.15$		Dislocation glide, twins, dislocation creep, microfracturing, some recrystallization
Quartz Diorite Wet-talc dehydration (Hansen, 1982; Hansen and Carter, 1982)	1000 MPa talc	creep tests $T = 758° - 956°C$ $\dot{\epsilon} = 2 \times 10^{-5} - 5 \times 10^{-7}\ s^{-1}$ $\Delta\sigma = 170-860$ MPa	$\log A = -1.5$ $Q_c = 212$ $n = 2.4$		semibrittle behavior Quartz—ductile deformation; feldspar—glide twins, and subgrains; pyroxenes—glide and microfracturing
Aheim and Anita Bay [3] Dunite Dry (Chopra and Paterson, 1984)	300 MPa gas	constant strain rate, $\dot{\epsilon}$-incremental $T = 1200° - 1400°C$ $\dot{\epsilon} = 10^{-4} - 10^{-6}\ s^{-1}$ $\Delta\sigma = 96-577$ MPa	$\log A = 4.5$ $Q_c = 535 \pm 33$ $n = 3.6 \pm 0.2$		dislocation glide, subgrain formation, grain boundary migration; local melt; microcracks

Aheim Dunite [3] Wet (0.1 wt.%) (Chopra and Paterson, 1981)	300 MPa gas	constant strain rate $T = 1000° - 1210°$ C $\dot{\epsilon} = 10^{-3} - 10^{-6}$ s^{-1} $\Delta\sigma = 112-740$ MPa	log $A = 2.6$ $Q_c = 498 \pm 38$ $n = 4.5 \pm 0.3$	dislocation glide, subgrain formation, dynamic recrystallization
Anita Bay Dunite [3] Wet (0.2 wt.%) (Chopra and Paterson, 1981)	300 MPa gas	constant strain rate $T = 1000° - 1300°$ C $\dot{\epsilon} = 10^{-3} - 10^{-6}$ s^{-1} $\Delta\sigma = 63-513$ MPa	log $A = 4.0$ $Q_c = 444 \pm 24$ $n = 3.35 \pm 0.2$	dislocation glide, subgrain formation, dynamic recrystallization
Mt. Burnet Dunite [3] Wet (Talc dehydration) (Post, 1973, 1977)	500 MPa talc	creep, stress relaxation σ, T-incremental $T = 759° - 1147°$ C $\dot{\epsilon} = 1.3 \times 10^{-3} - 3.6 \times 10^{-8}$ s^{-1} $\Delta\sigma = 269-828$ MPa	log $A = -2.5$ $Q_c = 392 \pm 22$ $n = 5.1 \pm 0.6$	dislocation glide, dislocation creep, dynamic recrystallization, ductile faulting

[1] All tests are in triaxial compression except Yule Marble (1) cylinders.

[2] Errors quoted as ± 2 standard deviations (i.e., 95% confidence limits)

[3] For extrapolations (Figs. 6–8), the more complete flow equation $\dot{\epsilon} = A \exp[-(Q_c + PV^*)/RT]\ \sigma^n$ was employed with the value of V^* (activation volume) taken as 17×10^{-6} m^3/mole (Kirby, 1983).

[4] Refit parameters: (A) *Anhydrite*—Müller and Briegel (1978) fitted their Riburg anhydrite data by a hyperbolic-sine function following Garofalo (1965). The power law shown in Table 4 is a standard transformation. (B) *Websterite (dry)*—Based on the values of flow parameters given by Avé Lallemant (1978), the calculated strain rates are about one order lower than the data points in Avé' Lallemant (1978, fig. 17). All data points in his fig. 17 are digitized and refitted by a multiple linear regression. (C) *Albite (dry) and Aplite (dry)*—The flow parameters were estimated separately by Shelton (1981). The stress exponent n for a given temperature was obtained from a plot of ln $\dot{\epsilon}$ vs. ln σ; the averaged n value for all temperatures was used. The activation energy Q for a given stress was obtained from a plot of ln $\dot{\epsilon}$ vs. $1/T$; the averaged value of Q under all stress conditions was used. We refit Shelton's data using simple multiple linear regression. (D) *Clinopyroxenite (dry)*—The original flow parameters were obtained using a method similar to that of Shelton's (1981). Instead of using ln $\dot{\epsilon}$ vs. $1/T$, Kirby and Kronenberg obtained Q by plotting ln σ vs. $1/T$ (Kirby and Kronenberg, 1984, fig. 10). We refit clinopyroxenite data under pressure 1500 ± 150 MPa by multiple linear regression. The data selected are not influenced by the transition: $\dot{\epsilon} \leqslant 10^{-7}$ s^{-1} for 800 °C, $\leqslant 10^{-6}$ s^{-1} for 900 °C, $\leqslant 10^{-4}$ s^{-1} for 985 and 1000 °C. The single 1100 °C data point (N318) is omitted.

values of the stress exponent, n, may eventually prove to be most important. Four sets of data have been refit using multiple linear regression (Table 4, footnote 4). The most difficult selection made, because of the several starting materials, flow laws, and varieties of techniques used was for quartzite deformed in solid pressure medium equipment. There is little basis for selection other than the requirement that the quartzite deformed dominantly in the α-quartz stability field; in any instance, the results of the several studies do not vary widely. Paterson (1987) has cautioned that extrapolations for quartz-rich rocks represent an upper bound on flow stress because influences of fugacity and of scale of dispersion of water are uncertain.

The most serious problem that has plagued experimentalists in this field has been the justification for extrapolations of empirical steady-state flow equations derived from laboratory mechanical experiments of practical durations (corresponding to strain rates $> 10^{-9}$ s^{-1}) to the much lower average strain rates of most natural deformations. Such justification is generally based on two sets of considerations: (1) high-temperature steady-state data for rocks generally fit a Weertman-type power-law flow equation (Table 4) as do metals and ceramics at similar values of normalized temperatures (T/T_m: homologous temperature) and stress (σ/E), where T_m (K) is the melting temperature and E is Young's Modulus. There is considerable support for an equation of this form from rate-process, dislocation and diffusion theory and observations (e.g., Dorn, 1954; Sherby and Burke, 1968; Weertman, 1968; Weertman and Weertman, 1975, 1983; Poirier, 1985); and (2) the observation, to the TEM level, that deformation mechanisms operative in the experiments are commonly virtually identical to those in rocks deformed naturally under inferred high temperature creep conditions.

Apart from problems such as scaling, discontinuities and fabric anisotropy, and known or perceived differences in boundary and environmental conditions between controlled laboratory experiments and natural deformations, important uncertainties are associated with direct application of observations from structurally relatively simple metals and ceramics to complex silicates. Among these are: (1) activation enthalpies and volumes for creep of metals and ceramics commonly correspond to those for self-diffusion (including core diffusion) of the least mobile atomic species (Dorn, 1954) whereas for silicates, for the few data available, such a correlation has not yet been established. This suggests that diffusion in silicates is much more complicated and/or that activation parameters for creep reflects significant contributions from other mechanisms; (2) dilatancy has been observed in natural rocksalt deformed experimentally under high-pressure, high-temperature, steady-state conditions (Wawersik and Hannum, 1979; Handin et al., 1986) and has been observed or calculated for high-temperature plasticity of other rocks (Fischer and Paterson, 1985; Boland and Tullis, 1986); and (3) some of the crystalline materials included in Table 4, all of which fit the Weertman relation well, are deformed in the semi-brittle regime, near the semi-brittle–ductile boundary.

Because measurements of dilatancy have not been technologically feasible in experiments done in solid-pressure medium apparatus, or in the high-temperature creep regime for silicates deformed in gas confining medium equipment, it is quite possible that crack-opening occurs in these experiments as well. Smith and Evans (1984) have shown that cracks in quartz heal rapidly in the presence of pore fluid, with an activation energy of 50 kJ/mol, and predict that such cracks would have geologically short lifetimes at temperatures above 200 °C. It is suggested that crack opening and healing may occur in silicates deformed in the high-temperature ductile regime, possibly at constant rates, and may contribute to the flow parameters determined from the mechanical data. While microcrack opening and healing processes may not occur, or may not be significant at low rates of natural deformations of silicates at high temperatures and pressures, they may well be important at effective pressures extant for continental crustal deformations. For these reasons, we conclude that extrapolations of high-temperature, steady-state creep data for silicates, deformed experimentally both in the ductile and semi-brittle regimes, provide only rough estimates of the actual flow stress

at depth; relative behaviors of various types of silicate rocks may be considerably more reliable. Extrapolations into grainsize-sensitive domains (Paterson, 1987) and generally out of their range of applicability form the basis for still greater uncertainty.

Steady-state flow stress–depth relations for continental lithosphere

Bearing the foregoing reservations in mind, we have extrapolated data included in Table 4 to strain rates of 10^{-15} s^{-1} (cratonic) and 10^{-14} s^{-1} (orogenic) using Mercier's (1980a) continental and oceanic geotherms (Fig. 4A), respectively, to obtain stress–depth profiles for the various materials. Figures 4C and 4D show such profiles for some shallow, non-silicate, rocks for which data are available; galena is included for comparison. The profiles are generally similar in the two regimes, the flow stress diminishing rapidly with depth and then bending rather gently (galena, Yule Marble, Carrara Marble, regime 2) or relatively abruptly (anhydrite, Solenhofen limestone) toward the depth axis at stresses < 10 MPa. Although the weakening effect of the steeper thermal gradient used for orogenic regions is partially compensated by the higher average strain rate adopted (see

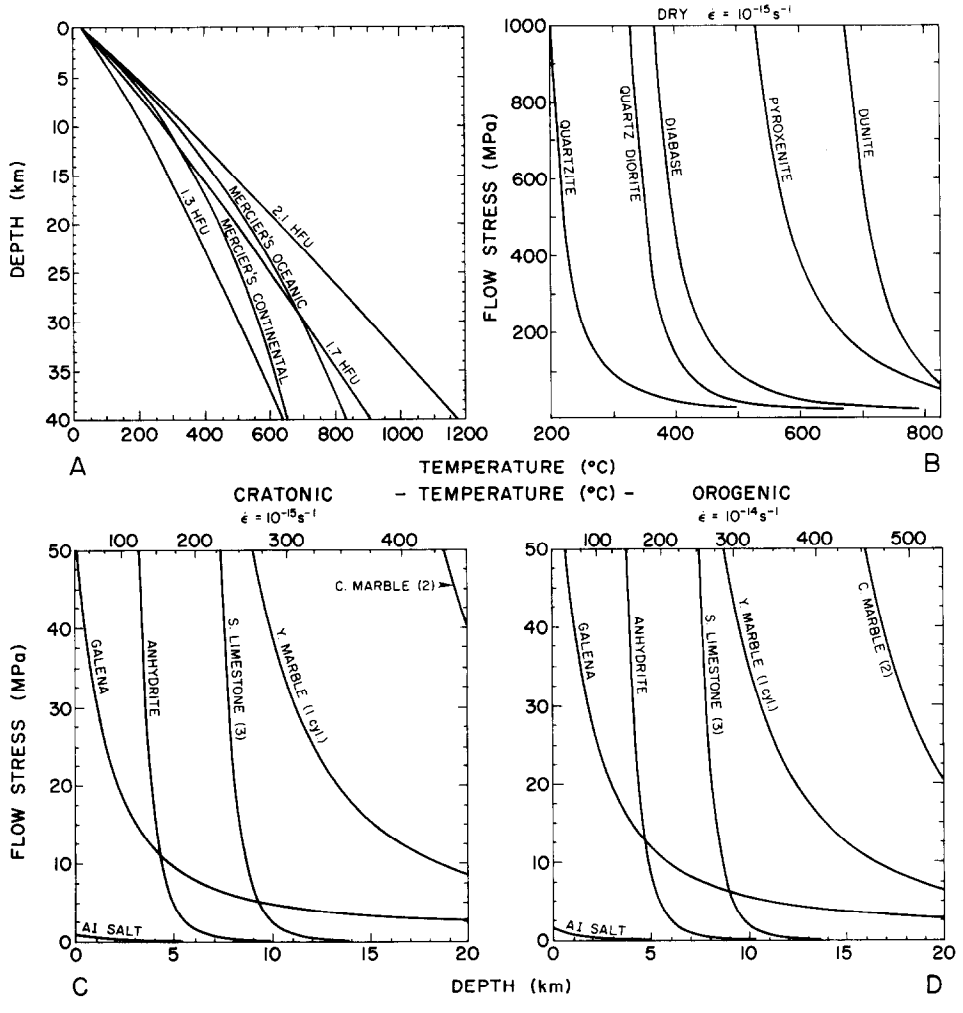

Fig. 4. A. Temperature–depth profiles from Lachenbruch and Sass (1977) and Mercier's (1980a) continental and oceanic geotherms. B. Temperature–flow stress profiles for selected continental crustal and upper mantle rocks (Kirby, 1985). C, D. Flow stress–depth profiles for non-silicate rocks deforming in the steady-state under model cratonic conditions (C—continental geotherm; $\dot{\epsilon} = 10^{-15}$ s^{-1}) and orogenic provinces (D—oceanic geotherm; $\dot{\epsilon} = 10^{-14}$ s^{-1}). See Table 4 for references and text for discussion.

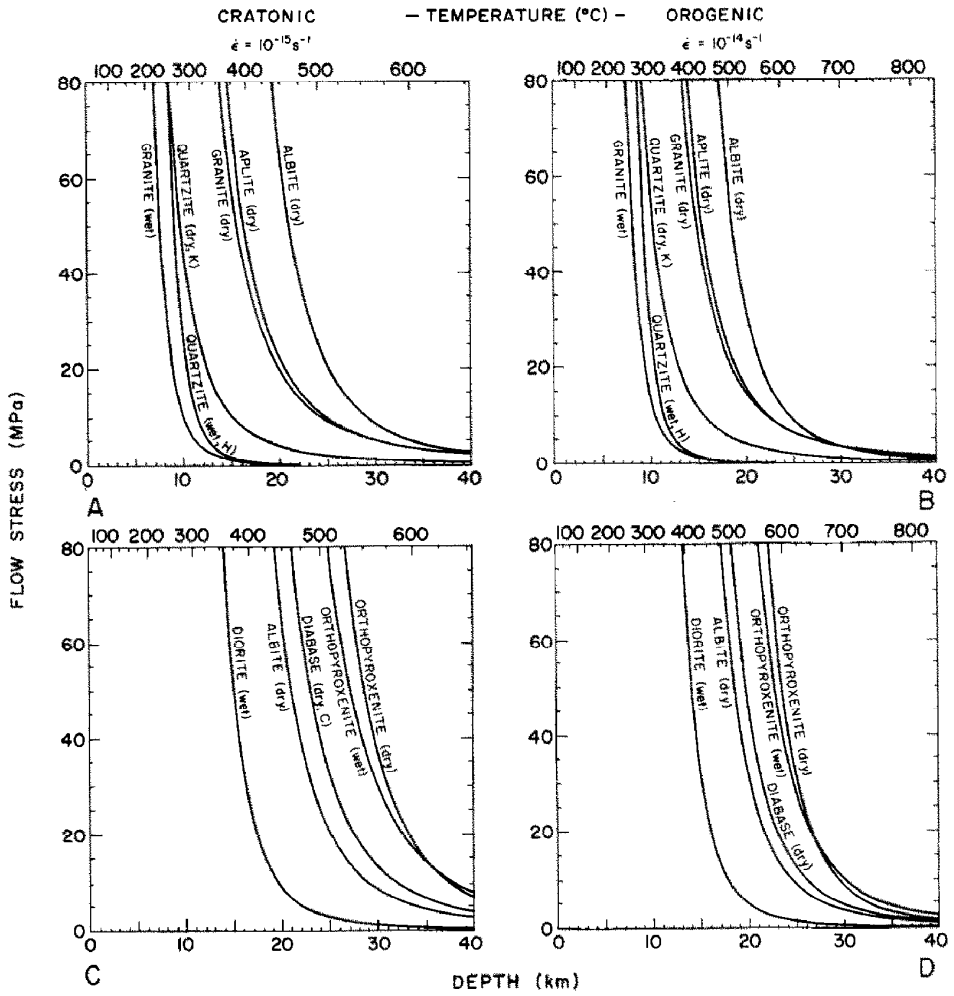

Fig. 5. Flow stress–depth (to 40 km) profiles for felsic (A, B) and mafic (C, D) rocks deforming in the steady state under model cratonic (A, C) and orogenic (B, D) regions. See Table 4 for references and text for discussion.

Kirby, 1985, fig. 3), the flow stress at a given depth is generally lower for all rocks considered, the decrease being strongly material-dependent.

Stress–depth profiles for felsic crystalline rocks (upper- to mid-crust) for the two thermal regimes are plotted in Figs. 5A and 5B and those for mafic rocks (mid- to lower-crust) are shown in Figs. 5C and 5D; albite rock is included in all four diagrams for comparison. As for the non-silicates, flow stresses for all the materials are strongly depth (temperature)-dependent to depths corresponding to flow stresses near 10 MPa where they bend abruptly toward the depth axis. This rather dramatic change takes place in the depth interval 10–15 km for quartzite and wet granite, 20–28 km for dry granite, aplite, albite rock and wet diorite, and 25–40 km for albite rock, diabase and orthopyroxenite. These depth intervals vary only slightly with tectonic province for the felsic rocks and somewhat more strongly, toward shallower depths in orogenic regions, for the mafic rocks.

Figures 6A and 6B show stress–depth profiles for selected mafic (websterite and clinopyroxenite) and ultramafic rocks at depths from 40 to 100 km for the two tectonic provinces. The profiles are generally more of the gradual-bending type and depths below which the flow stress falls below 10 MPa are quite strongly province-dependent. All curves (except dry clinopyroxenite) fall below 10 MPa flow stress at 60 km in orogenic regions whereas a depth of 85 km (except dry clinopyroxenite) is required for cratonic regions.

The stress–depth profiles in Figs. 5A, 5C and 6A ($\dot{\epsilon} = 10^{-15}$ s^{-1}) may be compared with stress–temperature profiles of Kirby (1985, fig. 5), reproduced here as Fig. 4B. The main differences in the two sets of profiles are the scales employed and non-linear temperature variation used in our diagrams. Kirby (1985) suggests that for each material, a critical temperature, T_c, exists at about 100 MPa flow stress, above which the predicted steady-state strength decreases abruptly with increasing temperature. For the crustal materials, T_c corresponds with weak zones and for mantle rocks, with the base of the lithosphere.We agree with this interpretation but, at the scale of our profiles, a stress level nearer 10 MPa, is indicated for the drastic weakening. Therefore, T_c is appreciably higher if our interpretation is more nearly correct, being about 950 °C at 85 km for the base of the lithosphere below cratons and about 1050 °C at 60 km below orogenic regions.

Flow stresses are not only strongly temperature-dependent but are also highly strain rate-dependent as is illustrated for mafic and ultramafic rocks at 40 km in Figs. 6C (cratonic; 654 °C) and 6D (orogenic; 832 °C). At constant temperature, the flow stress drops rapidly with decreasing strain rate as is particularly well-illustrated in Fig. 6C. For example, the flow strength of wet Aheim

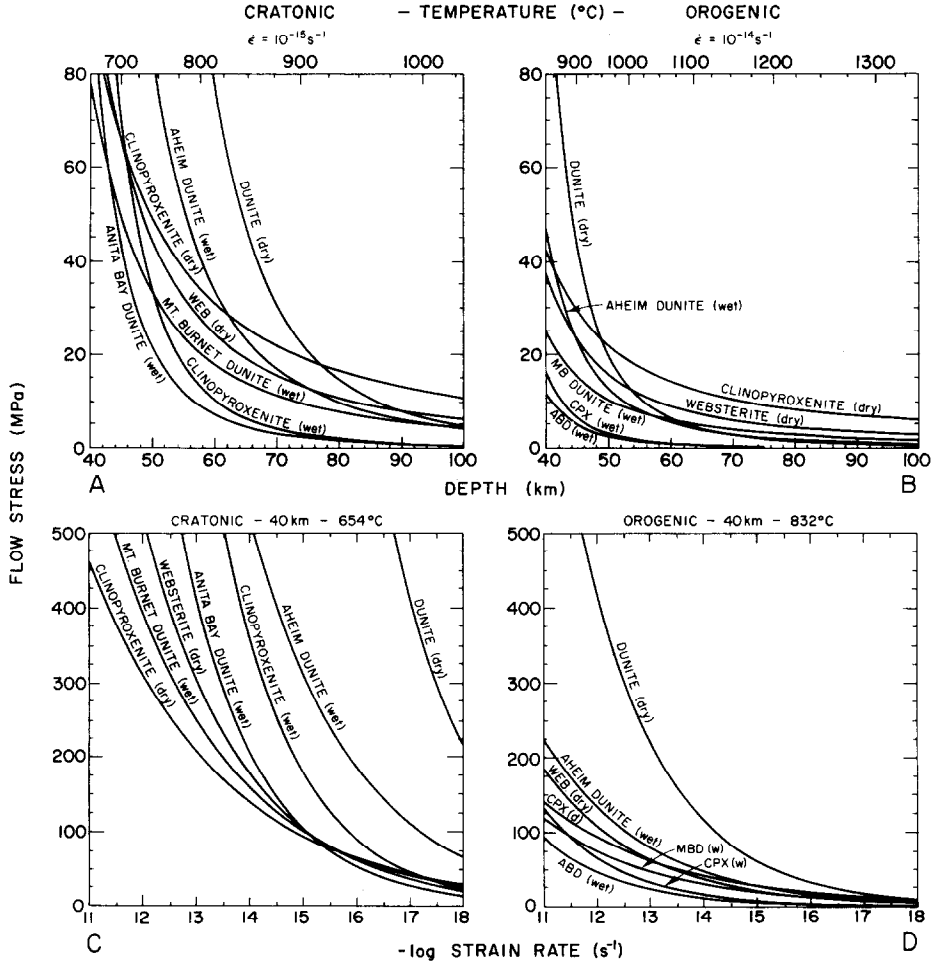

Fig. 6. Flow stress–depth (to 100 km) profiles for mafic and ultramafic rocks deforming in the steady state under model cratonic (A) and orogenic conditions (B). C, D. Flow stress–log strain rate profiles for constant temperatures of 654 °C and 832 °C at the base of 40 km crust assuming a continental geotherm (C) and oceanic geotherm (D).

dunite at 654° C is 500 MPa at 10^{-14} s^{-1}, dropping to about 70 MPa at 10^{-18} s^{-1} and at 832° C it is near 50 MPa at 10^{-14} s^{-1}, decreasing to about 5 MPa at 10^{-18} s^{-1}. More importantly (for reasons to be discussed below), because of the different temperature- and strain rate-dependencies of the various materials, some of the profiles shown in Fig. 6C change relative positions at the higher temperature (Fig. 6D). Dry dunite remains strongest but wet Aheim dunite has a flow strength near or below some of the mafic rocks at strain rates below about 10^{-14} s^{-1}. Anita Bay dunite has an intermediate flow strength at strain rates above 10^{-15} s^{-1} at 654° C (Fig. 6C) whereas it is weakest over the entire 7 decade strain rate range at 832° C (Fig. 6D).

Weak zones in the lithosphere and mechanical discontinuity at the Moho

Figure 7 is a summary plot showing steady-state flow stress–depth (temperature) relations for continental lithosphere of model cratonic and oceanic regions to a depth of 70 km. Beginning at the surface, Byerlee's relation (1968, 1978) may represent the rock-mass response of broken crystalline rocks to a maximum depth of 5 km whereupon frictional resistance is shown arbitrarily (dashed lines) to decrease nonlinearly with depth. For the remainder of the crust, average stress–depth profiles for materials selected from Fig. 5 are as shown. These steady-state profiles cannot continue indefinitely toward higher stresses at lower

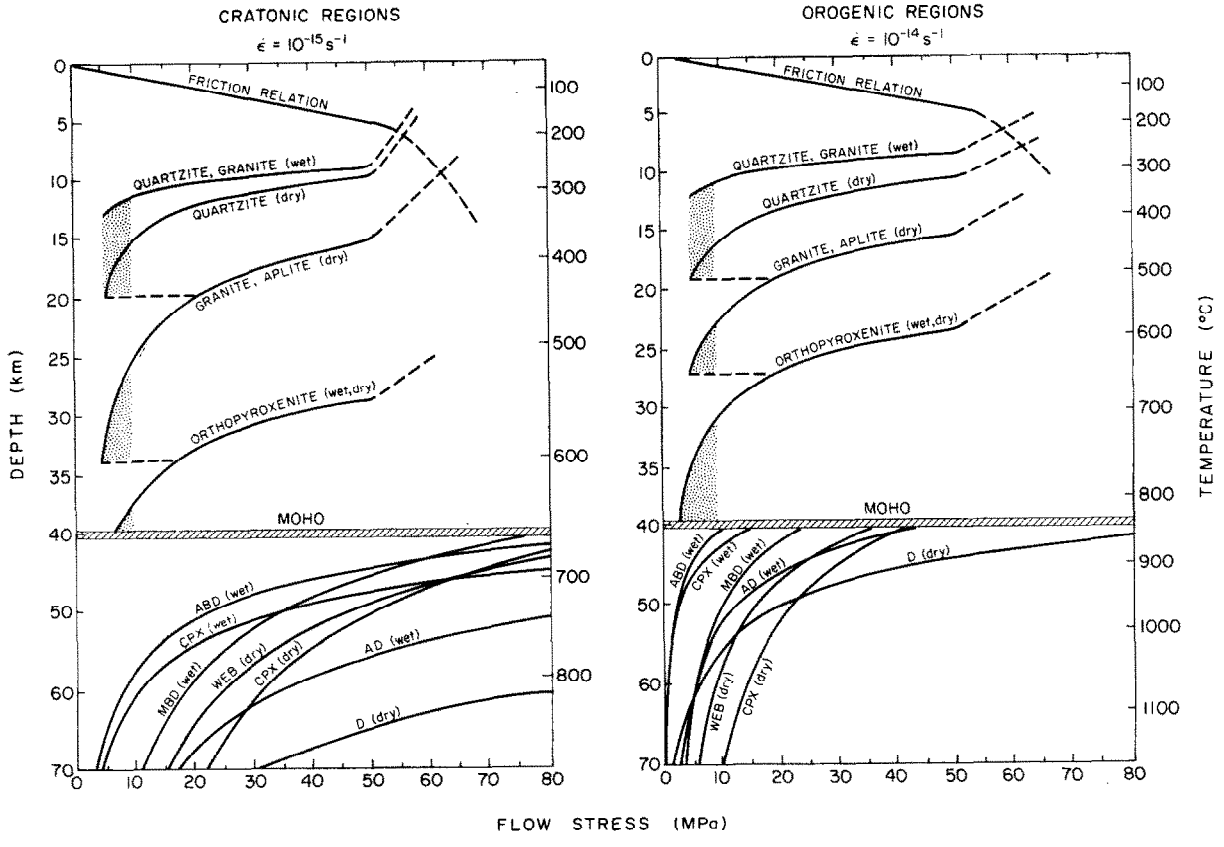

Fig. 7. Schematic diagram showing Byerlee's (1978) friction relation and various average steady-state flow stress profiles above the Moho for model cratonic and orogenic regions and profiles, below the Moho, for all mafic and ultramafic materials selected. Dashed lines in crustal portion indicate arbitrary depths and stresses for breakdown of the linear friction relation and of high-temperature steady-state flow laws. See text for discussion.

temperatures with decreasing depth and so are shown to break down to some other type of behavior (dashed lines), probably semi-brittle, at an arbitrarily chosen flow stress of 50 MPa. Stippled zones represent approximate depth intervals of weak zones in which the steady-state stress for the materials selected falls below 10 MPa.

Many scientists in recent years have suggested that the Moho represents a mechanical discontinuity with the underlying peridotite being appreciably stronger than the lower crust (e.g., Bird, 1978; Meissner and Strehlau, 1982; Chen and Molnar, 1983; Kirby, 1985; Zuber et al., 1986). Casual inspection of the profiles shown in Fig. 7 supports this notion but also shows that the magnitude of the discontinuity is likely to be highly temperature-dependent. It may be inferred from Figs. 6C and 6D that the magnitude is also strongly strain-rate-dependent. Furthermore, it is unlikely that the mechanical behavior of orthopyroxenite approximates that of a pyroxene–amphibole–plagioclase granulite which is believed to be more representative of the lower crust. Thus, although a mechanical discontinuity is likely to occur at the Moho, and the mantle below is probably *generally* stronger, both the nature and magnitude of the discontinuity are expected to vary laterally appreciably with constitution as well as physical/chemical environment associated with specific tectonic provinces. Recent studies of oceanic layer 3 gabbros within and above the Moho transition zone of the Samail, Zambales and Bay-of-Islands ophiolites indicate that the gabbros have undergone significant high-temperature ductile creep, as has the peridotite below (Wilks and Carter, 1986). These observations suggest that there may be no significant mechanical discontinuity for these high-temperature fragments of oceanic lithosphere.

Other mechanically weak zones that have received considerable attention in recent years are those that result from concentrated ductile and semi-brittle flow. The first of these produced experimentally and described clearly in the published literature (Blacic, 1972, fig. 2) occurred after 13% strain in nominally dry Mount Burnet dunite deformed at 1000 °C, 1500 MPa confining pressure at a strain rate of 10^{-4} s^{-1}. Blacic concludes that the instability occurs along a localized zone of shear and recrystallization promoted by weakening due to small amounts of water in the dunite. Post (1973) also produced ductile fault zones during high temperature creep of dunite and proposed that the mechanisms responsible for this behavior within the fine-grained fault zone, following reduction of grain size, might be grain-size sensitive. This suggestion has been developed further by Twiss (1977) who proposed a diffusion-accommodated, grain boundary sliding mechanism and by Goetze (1978) who proposed a "non-linear Coble" creep mechanism for both the ductile faulting and water-weakening of dunite. However, Zeuch (1982), in a critical analysis of evidence for the transition from dislocation creep to grainsize sensitive mechanisms, has shown that several observations are incompatible with such a transition and that dynamic recrystallization of hydrolytically-weakened olivine (Blacic, 1972), which requires no change in mechanism, is consistent with the available information.

More recently, ductile shear zones have been produced in experimentally deformed synthetic aggregates of albite by dynamic recrystallization-accommodated dislocation creep resulting in grainsize reduction and strain softening (Tullis and Yund, 1985). The small neoblasts have strong preferred orientations consistent with those observed in many mylonites and the authors conclude that similar microdynamic processes and strain softening may occur in ductile shear zones. Kirby (1985) points out that ductile shear zones have been produced experimentally in five different rock types and are generally associated mechanically with strain-softening in constant strain-rate tests or with accelerating creep in constant stress tests. In addition to hydrolytic weakening and dynamic recrystallization discussed above, Kirby cites hydrothermal alteration and phase changes during metamorphism as physical processes observed in experiments that may give rise to ductile faulting. He emphasizes the importance of aqueous solutions in most softening processes associated with ductile faulting and discusses the several physical mechanisms by which the finer grains observed in these shear zones may contribute to the softening.

Shelton et al. (1981) produced faults at high temperature and pressure in albite rock at stresses above and pressures below those at which hydrolytic weakening may occur. Apparently, the high temperature faults occur when there is sufficient dislocation mobility to accommodate only part of the deformation and to blunt crack tips; that is, the faulting mechanisms are semi-brittle. The sharp, apparently gouge-free, faults are inclined at angles near 45° to σ_1 and may propagate as shear cracks, tensile stress concentrations being reduced by high confining pressure and low, temperature-dependent, friction. The maximum value of the coefficient of friction, μ, observed in these experiments at 500 to 1500 MPa confining pressure and 700° to 1125°C is 0.4 (as compared to a minimum of 0.6 for Byerlee's relation) and is approximately 0.15 for tests at 900°C. The maximum value of the shearing stress, τ at 900°C at 1500 MPa confining pressure is 600 MPa as compared with 1300 MPa predicted by Byerlee's relation (Shelton et al., 1981).

White and White (1983), in their detailed study of microstructures within the Alpine fault zone, document all of the deformation mechanisms discussed above from cataclasis to dynamic recrystallization; i.e., from brittle to ductile faulting. They focus, however, on semi-brittle behavior observed in a broad transition of retrogressive metamorphism produced by sub-critical microcracking and fluid infiltration. Both ductile and brittle (stress corrosion cracking) processes operate cyclically and alternately in response to stress cycling following the initial phase of retrogression. The development of phyllosilicates during continued retrogression enhances increasing macroscopic ductile deformational behavior through time.

Hobbs et al. (1987) have questioned the common interpretations of coincidence of the seismogenic zone with the brittle–ductile transition on the basis of observations of pseudotachylites from a shear zone in Australia. They show that the pseudotachylites are generated in a cyclical manner and propose that they, and associated ultramylonites are instabilities developed entirely within the ductile field. On the basis of experimental and theoretical arguments concerning the velocity-dependence of frictional sliding, Hobbs et al. (1987) correlate the base of the continental seismogenic zone with the transition from velocity-weakening to velocity-strengthing, provided that the transition temperature is below a critical temperature, T_c (defined, at a given strain rate, as that at which the rate of transient work hardening equals the rate of stress relaxation due to shear heating and thermal fluctuations), a requirement for ductile instability.

Ord and Hobbs (1987), using an approach appreciably different from ours, arrive at virtually the same conclusions given in this and the Discussion section, although they prefer a somewhat higher breakdown stress for Beyerlee's law.

Flow in the upper mantle

The earth's upper mantle beneath both continental and oceanic crust is now widely acknowledged to be composed dominantly of peridotite, based on extensive observations of xenoliths, massifs and ophiolite sequences and on inferences drawn from density considerations, seismic body and surface wave velocities and on seismic anisotropy. The primary mineral composing peridotites is olivine (about Fo_{90}), generally with varying but lesser proportions of orthopyroxenes, clinopyroxenes, an aluminous phase (normally spinel or garnet) and accessory minerals. However, studies of upper mantle materials from depths to 250 km, above the olivine–spinel transition, indicate that the flow of olivine, in most instances, is responsible for most of the large-scale creep strain and that its internal deformation is probably generally rate-controlling. For this reason, the flow properties and processes of olivine crystals and aggregates deforming in the high-temperature ductile regime have received considerable attention in the past 20 yrs with the results of individual analyses generally converging toward a fundamental understanding of their behavior in this regime. Much less effort has been placed on elucidating the behavior of olivine single crystals and peridotites at low temperatures, studies that are likely to be important for sub-cratonic upper mantle and are certainly important for sub-oceanic upper mantle (Tsenn and Carter, 1987).

Low-temperature ductile and semi-brittle flow

Phakey et al. (1972) carried out six experiments on olivine single crystals of three orientations at 1000 MPa confining pressure, 600° and 800°C, at strain rates of 10^{-4} and 10^{-5} s^{-1}. They observed maximum values of $(\sigma_1 - \sigma_3)$ ranging from 520 to 1280 MPa under these conditions and observed, using TEM, conservative motion of dislocations in general at 600°C and that cross slip occurs at 800°C. Kirby (1980) cites unpublished data on low-temperature ductile flow of Balsam Gap dunite at 1500 MPa confining pressure in which the flow stress dependence on strain rates, in the range 10^{-3} to 10^{-6} s^{-1}, was determined at 600°C and the temperature sensitivity of strength was determined at 10^{-5} s^{-1} over the range 400° to 900°C. Both the temperature and strain rate sensitivities of strength were found to be small, very similar to clinopyroxenite, and Kirby predicts a low-temperature to high-temperature transition stress, σ_b, of about 1400 MPa at a strain rate of 10^{-14} s^{-1}, noting that this is likely to be an underestimate because of the work-hardening nature of the experiments. Based on these arguments, Kirby (1983) modified Goetze and Evan's (1979) yield envelope to incorporate low-temperature ductile and semi-brittle behavior (Fig. 2B). Although poorly-constrained, this modification is appreciable; however, the stress levels, even for the flexure problem addressed, are still very high.

High-temperature ductile flow

The high-temperature flow of various starting materials, the deformation equipment used to investigate this field experimentally and microstructural analyses have been discussed and reviewed many times in the last decade (e.g., Nicolas and Poirier, 1976; Carter, 1976; Kohlstedt et al., 1976; Ashby and Verrall, 1978; Mercier et al., 1977; Durham and Goetze, 1977a, b; Goetze, 1978; Weertman, 1978; Goetze and Evans, 1979; Kirby, 1977, 1980, 1983, 1985; Avé Lallemant et al., 1980; Mercier, 1980b; Chopra and Paterson, 1981, 1984; Karato, 1984; Zeuch and Green, 1984a, b; Poirier, 1985; Mackwell et al., 1985; Chopra, 1986; Freund and Oberheuser, 1986; Karato et al., 1986; Tullis and Horowitz, 1987; Tsenn and Carter, 1987), obviating the need for a summary here. We have adopted the "wet" and "dry" results primarily on Aheim (0.9 mm grain size) dunite (Table 4) of Chopra and Paterson (1981, 1984), carried out in gas apparatus at 300 MPa confining pressure, as representative of the flow properties of the upper mantle. The wet experiments (> 0.1 wt.% H_2O), defined by presence of small amounts of water from initially hydrous minerals, were carried out at temperatures from 1000° to 1300°C at strain rates from 10^{-3} to 10^{-6} s^{-1} with the resulting near-steady-state flow stresses ranging from about 150 to 700 MPa. Dry (< 0.003 wt.% H_2O) experiments, using samples heat-treated at 1200°C for > 60 hrs in a controlled oxygen fugacity furnace, were performed in the temperature range 1200° to 1400°C, strain rates from 10^{-4} to 10^{-6} s^{-1} with steady state stresses ranging from about 100 to 600 MPa. The dried samples, at a given stress level deform at strain rates 1 to 2 orders of magnitude lower than the wet ones and the strength dependence of grain size (comparing Anita Bay dunite with 0.1 mm grainsize) observed in the wet experiments disappears in dried specimens, both materials giving the same flow law (Table 4). *Most importantly*, the presence of as little as 0.01 wt.% H_2O added to the pre-dried specimens lowers the strength to stress levels comparable with wet specimens (Chopra and Paterson, 1984, fig. 11).

Optically observed textures and microstructures in olivine of the wet specimens progress with increasing temperature at a strain rate of 10^{-5} s^{-1} from strong flattening of grains with serrated boundaries containing deformation lamellae and kink bands, to the disappearance of lamellae and appearance of undulatory extinction, subgrain development, grain boundary recrystallization, and a more equant grain morphology (Chopra and Paterson, 1981). The general trends shown for a similar progression in conditions for dry specimens begin with kink bands, giving way to undulatory extinction and subgrain development; grain boundaries show evidence of mobility at the higher temperatures but recrystallization is not observed (Chopra and Paterson, 1984). Axial extension fractures occur in both wet and dry Aheim dunite

deformed at the higher stress levels (lower temperatures and higher strain rates) and Chopra and Paterson allow that at higher confining pressures (required to suppress such fracturing) the flow strength would probably be somewhat higher.

The same general progression of microstructural development described above has also been observed in several other optical studies of experimentally deformed olivine and such structures are also typical of naturally deformed peridotites; this correlation has also been extended to the scale of TEM observations. Because of the low confining pressures applied, and consequent development of microfractures, we may regard deformation at higher stresses as semi-brittle; this raises some concern about the general applicability of the flow laws derived by Chopra and Paterson (1981, 1984). However, the wet results for Aheim dunite are in close accord with single crystal data for $[110]_c$ and $[101]_c$ orientations (Durham and Goetze, 1977a, fig. 5). Dry results correspond closely to those for single crystals of $[011]_c$ orientation, experiments on Balsam Gap and synthetic dunites (Tullis and Horowitz, 1987), and the flow parameters (Table 4) are nearly identical to those estimated by Kirby (1983, table 1) in his analysis of most available single and polycrystal data. The dry Aheim dunite results (Chopra and Paterson, 1984, fig. 13) also nearly coincide with the original results of Carter and Avé Lallemant (1970) although the coincidence is regarded as fortuitous (Chopra and Paterson, 1984; Tullis and Horowitz, 1987), being ascribed to offsetting effects of weak samples and the strong confining medium (one of us (NLC) prefers the phrase "pioneering insight" to "offsetting effects"; he is, nonetheless, grateful that analyses based on the original data have not required appreciable modification).

The large difference in relative strength between wet and dry dunite may be highly significant as dry dunite is appreciably stronger, over a wide range of conditions (Figs. 6 and 7) than the commonly associated pyroxenes and pyroxenites. Extensive textural and microstructural studies of peridotite xenoliths and ultramafic suites in ophiolite sequences and Alpine massifs have invariably demonstrated that olivine is much more highly deformed, and hence weaker, than the pyroxenes (e.g., Mercier and Nicolas, 1975; Nicolas and Poirier, 1976; Mercier, 1977; Avé' Lallemant et al., 1980). These observations are inconsistent with the dry results for olivine; however, if only 100 ppm water is present in the olivine crystal structure, the mechanical behavior of olivine is virtually identical to that of wet dunite (Chopra and Paterson, 1984). Thus, we believe that the wet Aheim dunite flow law is that currently most representative of high temperature creep of the upper mantle beneath both continents and ocean basins and hence is most appropriate for analyses of upper mantle mechanical behavior.

Both Mercier (1980b) and Avé Lallemant et al. (1980) used paleostresses obtained from olivine recrystallized grainsizes (Ross et al., 1980) temperatures and pressures determined from pyroxene thermobarometry (Mercier, 1980a), along with Post's (1977) dry dunite flow law to calculate strain rates and viscosities as a function of depth for several tectonic provinces. However, the validity of Post's dry flow law is now in serious question (e.g., Tullis and Horowitz, 1980, 1987; Chopra and Paterson, 1984), yielding unreasonably high flow stresses at given strain rates and temperatures. Therefore, we have replotted in Fig. 8A the variation in strain rate beneath the South African craton, using the stress and depth (pressure, temperature) estimates of Avé Lallemant et al. (1980; table II, ICa, b) and wet and dry flow laws of Chopra and Paterson. The strain rate so obtained increases rapidly from about 10^{-17} s^{-1} at a depth of 75 km to about 10^{-15} s^{-1} at about 100 km and then more gradually to 10^{-12} s^{-1} at 240 km, with a break in slope and data in the depth range 110 to 160 km. Mercier (1980b) interprets this break as a change in recrystallization mechanism (Poirier and Nicolas, 1975), but Karato (1984) interprets it as recording the thermomechanical history of the xenoliths. The effect on calculated strain rates (Fig. 8A) and equivalent viscosities (Fig. 8B) in the depth range 100 to 400 km using wet and dry flow laws is minor, primarily because of the different temperature sensitivities of the two laws.

Figure 8B shows the variation in equivalent viscosity ($\eta = \sigma/3\dot{\epsilon}$) with depth using Chopra and Paterson's dunite flow equations, Mercier's (1980a) continental and oceanic geotherms and strain rates

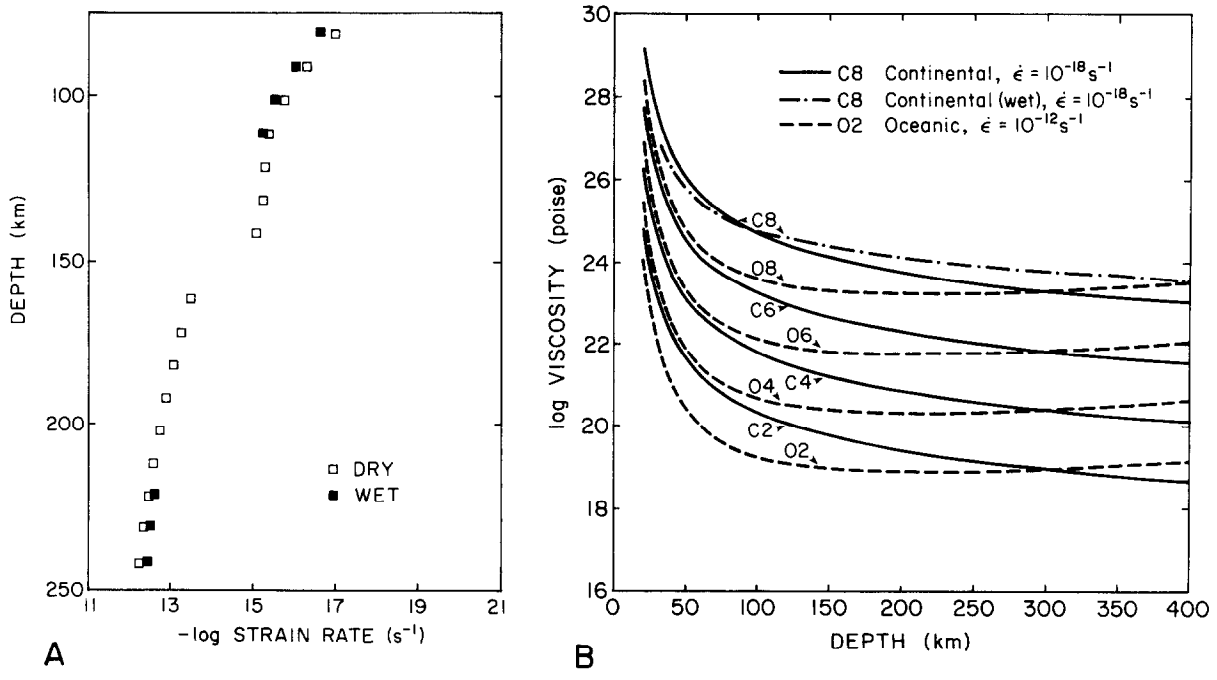

Fig. 8. Variation of strain rate with depth below 75 km estimated using stresses and depth beneath the South African craton from Avé Lallemant et al. (1980), and wet and dry flow laws of Chopra and Paterson (1981, 1984). B. Variation in equivalent viscosity with depth at various strain rates, calculated using Chopra and Paterson's (1981, 1984) flow equations for dunite and Mercier's (1980a) continental and oceanic geotherms.

in the range 10^{-12} to 10^{-18} s^{-1}. All viscosities drop sharply to a depth of about 50 km, those of oceanic regions flattening near 100 km and remaining constant thereafter to 400 km, whereas those for stable continental regions drop gradually. Sub-oceanic viscosities are about one order of magnitude lower than those under continental regions for mantle deforming at the same strain rate but the two intersect near 300 km depth because of variations in slopes of the geotherms. Average values for oceanic and continental regions, over the depth range 100 to 400 km (ignoring the olivine–spinel transformation) are a little lower than 10^{21} Poise at a strain rate of 10^{-14} s^{-1} and about 10^{22} Poise at 10^{-16} s^{-1}, values that are in reasonable accord with other geophysical considerations.

Discussion and conclusions

The likely occurrence of mechanically weak zones at depths below about 10 km in continental crust, suggested by the steady-state data available for crystalline rocks is strongly supported by geological and geophysical observations, some of which were alluded to in context above. Considered together with semi-brittle and ductile faulting, such weak zones may occur at virtually any depth in the continental lithosphere, depending on lithology, tectonic province and physical/chemical environment permitting or leading to large-scale extension décollement, decoupling, or detachment (e.g., Armstrong and Dick, 1974).

As pointed out by Sibson (1983), it is now widely recognized that thrust faults involving crystalline basement commonly flatten with depth into décollement zones at mid- to lower-crustal depths. An excellent example of this is provided by an interpretative cross section through the Alps showing basement–cover relations of the Glarus thrust and thick slices of the Aar, Tavetsch and Gotthard massifs (Pfiffner, 1985, fig. 10). Interesting contrasts in behavior are revealed by detachments beneath Shuswap complex in Canada (Armstrong, 1982), the relatively flat-lying 6–15 km crystalline allochton overthrusting 260 km of a

sedimentary sequence in the southern Appalachians and the uniformly-dipping (35°) Wind River thrust which apparently penetrates the entire crust. J.V. Ross (pers. commun., 1986) suggests that such fold and thrust belts develop by advances of thermal fronts which then, through dewatering, give rise to H_2O fronts permitting fluid migration. In accordance with our views, he believes that virtually all deformation in crustal crystalline rocks is dominated by semi-brittle mechanisms at all scales and that fluid-enhanced grain boundary diffusion processes are most important.

The situation for strike-slip faults is more complicated with possibilities ranging from penetration downward into the semi-brittle and ductile regime, through widening at the base of the frictional regime to spreading into a decoupled horizontal shear zone. Apparently, geological evidence suggests that the last of these alternatives is uncommon but that at least some shear zones do broaden with depth (Sibson, 1983).

Eaton (1980) and Smith and Bruhn (1984) have summarized the general geological and geophysical characteristics of the crust of the Basin and Range Province. Conceptual and observational models proposed for the large scale extension observed call variously for initial listric fault development, high-angle planar faults rotating to shallower dips during thinning through time, large scale extension along low-angle normal faults and/or temporal combinations of these (Morton and Black, 1975; Wernicke and Burchfiel, 1982; Jackson and McKenzie, 1983; Smith and Bruhn, 1984). In all instances, however, mechanically weak, ductile, or mylonitic zones are required at upper- to mid-crustal depths, zones which may be related in some manner to the Cordilleran core complexes (Coney, 1980); although temporal relations are not yet firmly established (Armstrong, 1982).

Theoretical mechanical models involving the development of regularly-spaced, boudinage-like instabilities, have been developed making use of available laboratory data (Fletcher and Hallet, 1983; Zuber et al., 1986; Froidevaux, 1986). The model of Fletcher and Hallet (1983) predicts uniformly spaced regions of enhanced extension (basins) alternating with regions of reduced extension (ranges) with a spacing near that observed, in the Basin and Range Province of Nevada if a weak zone occurs at 10 km depth. The more recent model of Zuber et al. (1986) predicts, in addition to the basin-and-range spacing, a longer wavelength instability which they correlate with the width of tilt domains, both instabilities arising from the presence of a strong upper crust and upper mantle separated by a weak lower crust. Froidevaux (1986) predicts boudinage-like instabilities in the upper mantle beneath the Basin and Range to provide thermal variations required to account for 200-km wavelength Bouguer gravity anomalies and COCORP seismic reflection data. Finally, Reiter and Minier (1985) have suggested that thermal stresses may have combined with regional tectonic stresses to help promote development of large-scale structures observed in the Basin and Range Province.

In summary, preliminary laboratory mechanical data generally appear to be in accord with many geological and geophysical observations and indeed have been utilized extensively to model the origin and evolution of lithospheric structures. Clearly, yield envelopes of the type first developed by Goetze and Evans (1979) provide useful information on the depth-dependence of flow stress; their continuing development and modifications for common lithospheric rocks, including composite polycrystals with textural and structural anisotropies, is essential. Similarly, concomitant development and refinement of deformation maps (Stocker and Ashby, 1973) or surfaces will establish a firm physical basis for construction of the envelopes as well as providing an essential link for interpretations of natural deformation processes. Particularly important in these ongoing laboratory studies are modifications of rock friction relations, delineations of boundaries between brittle, semi-brittle and ductile regimes, determinations of grainsize-sensitive domains and processes, and evaluations of depth-dependencies of these relations on the first-order physical and chemical variables.

Acknowledgements

The authors wish to acknowledge stimulating discussions with R. Carlson and S. Uyeda which led to our undertaking this analysis. We are grateful to F. Chester, A. Huffman, K. Wilks and especially to J. Handin, A. Kronenberg, M. Paterson, A. Pfiffner, J. Ross and D. Wiltschko for review of the manuscript and for many constructive suggestions for improvements. This research was supported by National Science Foundations Grants MSM-8413974 and OCE-8468050 and Department of Energy Project DOE-BES D6-F606-84ER13216.

References

Aines, R.O., Kirby, S.H. and Rossman, G.R., 1984. Hydrogen speciation in synthetic quartz. Phys. Chem. Miner., 11: 204–212.

Armstrong, R.E., 1982. Cordilleran metamorphic core complexes—from Arizona to southern Canada. Annu. Rev. Earth Planet. Sci., 10: 129–154.

Armstrong, R.E. and Dick, H.J.B., 1974. A model for the development of thin overthrust sheets of crystalline rock. Geology, 2: 35–40.

Ashby, M.F. and Verrall, R.A., 1978. Micromechanisms of flow and fracture, and their relevance to the rheology of the upper mantle. Philos. Trans. R. Soc. London, Ser. A., 288: 59–95.

Atkinson, B.K., 1976. The temperature- and strain-rate dependent mechanical behavior of a polycrystalline galena ore. Econ. Geol., 71: 513–525.

Atkinson, B.K., 1984. Subcritical crack growth in geological materials. J. Geophys. Res., 89: 4077–4114.

Avé Lallemant, H.G., 1978. Experimental deformation of diopside and websterite. Tectonophysics, 48: 1–27.

Avé Lallemant, H.G., Mercier, J-C.C., Carter, N.L. and Ross, J.V., 1980. Rheology of the upper mantle: inferences from peridotite xenoliths. Tectonophysics, 70: 85–113.

Bird, P., 1978. Initiation of intracontinental subduction in the Himalayas. J. Geophys. Res., 83: 4975–4987.

Blacic, J.D., 1972. Effect of water on the experimental deformation of olivine. Geophys. Monogr., Am. Geophys. Union, 16: 109–115.

Blacic, J.D., 1975. Plastic deformation mechanisms in quartz: the effect of water. Tectonophysics, 27: 271–294.

Blacic, J.D., 1981. Water diffusion in quartz at high pressure: tectonic implications. Geophys. Res. Lett., 8: 721–723.

Blacic, J.D. and Christie, J.M., 1984. Plasticity and hydrolytic weakening of quartz single crystals. J. Geophys. Res., 89: 4223–4240.

Boland, J.N. and Tullis, T.E., 1986. Deformation behavior of wet and dry clinopyroxenite in the brittle to ductile transition region. Geophys. Monogr., Am. Geophys. Union, 36: 35–50.

Brace, W.F., 1972. Pore pressure in Geophysics. Geophys. Monogr., Am. Geophys. Union, 16: 265–274.

Brace, W.F., 1980. Permeability of crystalline and argillaceous rocks. Int. J. Rock Mech. Min. Sci., 17: 241–251.

Brace, W.F., 1984. Permeability of crystalline rocks: new in situ measurements. J. Geophys. Res., 89: 4327–4330.

Brace, W.F. and Kohlstedt, D.L., 1980. Limits on lithospheric stress imposed by laboratory experiments. J. Geophys. Res., 85: 6248–6252.

Brodie, K.H. and Rutter, E.H., 1985. On the relationship between rock deformation and metamorphism with special reference to the behavior of basic rocks. In: A.B. Thompson and D.C. Robie (Editors), Advances in Physical Chemistry, 4. Springer, New York, N.Y., pp. 138–139.

Brodie, K.H. and Rutter, E.H., 1987. Deep crustal extensional faulting in the Irrea zone, Northern Italy. Tectonophysics, in press.

Byerlee, J.D., 1968. Brittle–ductile transition in rocks. J. Geophys. Res., 73: 4741–4750.

Byerlee, J.D., 1978. Friction of rocks. Pure Appl. Geophys., 116: 615–626.

Caristan, Y., 1980. High temperature mechanical behavior of Maryland Diabase. Ph. D. Thesis, MIT, Cambridge, Mass., 155 pp.

Caristan, Y., 1982. The transition from high-temperature creep to fracture in Maryland diabase. J. Geophys. Res., 87: 6781–6790.

Carter, N.L., 1976. Steady state flow of rocks. Rev. Geophys. Space Phys., 14: 301–360.

Carter, N.L. and Avé Lallemant, H.G., 1970. High temperature flow of dunite and peridotite. Geol. Soc. Am. Bull., 81: 2181–2202.

Carter, N.L. and Kirby, S.H., 1978. Transient creep and semibrittle behavior of crystalline rocks. Pure Appl. Geophys., 116: 807–839.

Carter, N.L. and Uyeda, S. (Editors), 1985. Collision Tectonics: Deformation of Continental Lithosphere. Tectonophysics, 119 (Special Issue): 449 pp.

Carter, N.L., Baker, D.W. and George, R.P., Jr., 1972. Seismic anisotropy, flow and constitution of the upper mantle. Geophys. Monogr., Am. Geophys. Union, 16: 167–190.

Carter, N.L., Anderson, D.A., Hansen, F.D. and Kranz, R.L., 1981. Creep and creep rupture of granitic rocks. Geophys. Monogr. Am. Geophys. Union, 24: 61–82.

Cathles, L.M., III, 1975. The Viscosity of the Earth's Mantle. Princeton Univ. Press, Princeton, N.J., 386 pp.

Chen, W-P. and Molnar, P., 1983. Focal depths of intracontinental and intraplate earthquakes and their implications for the thermal and mechanical properties of the lithosphere. J. Geophys. Res., 88: 4183–4214.

Chester, F.M., 1985. Correlation of halite gouge rupture with sliding mode and velocity dependence in experimental faults(abs). Eos, Trans. Am. Geophys. Union, 66: 1100–1101.

Chopra, P.N., 1986. The plasticity of some fine-grained aggregates of olivine at high pressure and temperature. Geophys. Monogr., Am. Geophys. Union, 36; 25–33.

Chopra, P.N. and Paterson, M.S., 1981. The experimental deformation of dunite. Tectonophysics, 78: 453–473.

Chopra, P.N. and Paterson, M.S., 1984. The role of water in the deformation of dunite. J. Geophys. Res., 89: 7861–7876.

Christie, J.M. and Ord, A., 1980. Flow stress from microstructures of mylonites: example and current assessment. J. Geophys. Res., 85: 6253–6262.

Clark, S.P., Jr. and Ringwood, A.E., 1964. Density distribution and constitution of the mantle. Rev. Geophys., 2: 35–88.

Coney, P.J., 1980. Cordilleran metamorphic core complexes: an overview. In: M.D. Crittenden, P.J. Coney and G.H. Davis (Editors), Cordilleran Metamorphic Core Complexes. Mem. Geol. Soc. Am., 153: 7–31.

Crittenden, M.D., Jr., 1967. Viscosity and finite strength of the mantle as determined from water and ice loads. Geophys. J.R. Astron. Soc., 14: 261–279.

Dahlen, F.A., 1984. Noncohesive critical Coulomb wedges: an exact solution. J. Geophys. Res., 89: 10, 125–10, 133.

Dahlen, F.A., Suppe, J. and Davis, D., 1984. Mechanics of fold-and-thrust belts and accretionary wedges: cohesive Coulomb theory. J. Geophys. Res., 89: 10,087–10,101.

Davies, G.F., 1980. Mechanics of subducted lithosphere. J. Geophys. Res., 85: 6304–6318.

Davis, D., Suppe, J. and Dahlen, F.A., 1983. Mechanics of fold-and-thrust belts and accretionary wedges. J. Geophys. Res., 88: 1153–1172.

Dieterich, J.H. and Conrad, G., 1984. Effect of humidity on time- and velocity-dependent friction in rocks. J. Geophys. Res., 89: 4196–4202.

Dorn, J.E., 1954. Some fundamental experiments on high temperature creep. J. Mech. Phys. Solids, 3: 85–116.

Dula, F., 1985. High temperature deformation of wet and dry artificial quartz gouge. Ph. D. Thesis, Texas A & M University, College Station, Tex., 382 pp.

Durham, W.B. and Goetze, C., 1977a. Plastic flow of oriented single crystals of olivine, 1. Mechanical data. J. Geophys. Res., 82: 5737–5753.

Durham, W.B. and Goetze, C., 1977b. A comparison of creep properties of pure forsterite and iron bearing olivine. Tectonophysics, 40: 15–18.

Eaton, G.P., 1980. Geophysical and geological characteristics of the crust of the Basin and Range Province. In: Continental Tectonics. Nat. Acad. Sci., Washington, D.C., pp. 96–113.

Etheridge, M.A., Wall, V.J. and Cox, S.F., 1984. High fluid pressures during regional metamorphism and deformation: implications for mass transport and deformation mechanisms. J. Geophys. Res., 89: 4344–4358.

Fischer, G.J. and Paterson, M.S., 1985. Dilatancy and permeability in rock during deformation of high temperature and pressure. Eos, Trans. Am. Geophys. Union, 66: 1065 (Abstr.).

Fletcher, R.C. and Hallet, B., 1983. Unstable extension of the lithosphere: a mechanical model for Basin-and-Range structure. J. Geophys. Res., 88: 7457–7466.

Forsythe, D.W., 1985. Subsurface loading and estimates of the flexural rigidity of continental lithosphere. J. Geophys. Res., 90: 12,623–12,632.

Fountain, D.M. and Salisbury, M.H., 1981. Exposed cross-sections through the continental crust: implications for crustal structure, petrology and evolution. Earth Planet. Sci. Lett., 56: 263–277.

Freund, F. and Oberheuser, G., 1986. Water dissolved in olivine: a single-crystal infrared study. J. Geophys. Res., 91: 745–761.

Friedman, M. and Higgs, N.G., 1981. Calcite fabrics in experimental shear zones. Geophys. Monogr., Am. Geophys. Union, 24: 11–27.

Friedman, M., Handin, J., Higgs, N.G. and Lantz, J.R., 1979. Strength and ductility of four dry igneous rocks at low pressures and temperatures to partial melting. Rock Mech. Symp., 20th, Austin, Tex., pp. 35–43.

Friedman, M., Handin, J., Bauer, S.J., Choi, Y.J., Hopkins, T.W. and Shimamoto, T., 1984. Mechanical properties of rocks at high temperatures and pressures. Proj. Rep. 1, D.O.E. Grant DE-FG05-84ER13228.

Froidevaux, C., 1986. Basin and Range large-scale tectonics: Constraints from gravity and reflection seismology. J. Geophys. Res., 91: 3625–3632.

Fyfe, W.S., Price, N.J. and Thompson, A.B., 1978. Fluids in the Earth's Crust. Elsevier, Amsterdam, 383 pp.

Gandais, M. and Willaime, C., 1984. Mechanical properties of feldspars. In: W.L. Brown (Editor), Feldspars and Feldspathoids. Reidel, Dordrecht, pp. 207–246.

Garotalo, F., 1965. Fundamentals of Creep and Creep-Rupture in Metals. Macmillan, New York, 258 pp.

Giletti, B.J. and Yund, R.A., 1984. Oxygen diffusion in quartz. J. Geophys. Res., 89: 4039–4046.

Gilluly, J., 1972. Tectonics involved in the evolution of mountain ranges. In: E.C. Robertson (Editor), The Nature of the Solid Earth. McGraw-Hill, New York, N.Y., pp. 406–439.

Goetze, C., 1978. The mechanisms of creep in olivine. Philos. Trans. R. Soc. London, Ser. A, 288: 99–119.

Goetze, C. and Evans, B., 1979. Stress and temperature in the bending lithosphere as constrained by experimental rock mechanics. Geophys. J.R. Astron. Soc., 59: 463–478.

Green, H.W., II, 1984. "Pressure solution" creep: some causes and mechanisms. J. Geophys. Res., 89: 4313–4318.

Griggs, D.T., 1972. The sinking lithosphere and the focal mechanisms of deep earthquakes. In: E.C. Robertson (Editor), The Nature of the Solid Earth. McGraw-Hill, New York, N.Y., pp. 361–384.

Griggs, D.T. and Handin, J., 1960. Observations on fracture and a hypothesis of earthquakes. Geol. Soc. Am. Mem., 79: 347–364.

Guffanti, M. and Nathenson, M., 1980. Preliminary map of temperature gradients in the conterminous United States. Geothermal Resour. Counc., Trans., 4: 53–56.

Haimson, B.C. and Doe, T.W., 1983. State of stress, permeability and fractures in the Precambrian granite of Northern Illinois. J. Geophys. Res., 88: 7355–7371.

Handin, J., 1966. Strength and ductility. Geol. Soc. Am. Mem., 97: 223–289.

Handin, J. and Carter, N.L., 1980. Rheology of rocks at high

temperature. Proc. 4th Congr. Int. Soc. Rock Mechanics, 3: 97–106.

Handin, J. and Raleigh, C.B., 1972. Manmade earthquake and earthquake control. Symp. Percolation Through Fissured Rock. Int. Soc. Rock Mechanics, Stuttgart, T2-D, 1–10.

Handin, J., Hager, R.V., Jr., Friedman, M. and Feather, J.N., 1963. Experimental deformation of sedimentary rocks under confining pressure: pore pressure tests. Am. Assoc. Pet. Geol. Bull., 47: 717–755.

Handin, J., Russell, J.E. and Carter, N.L., 1986. Experimental deformation of rocksalt. Geophys. Monogr., Am. Geophys. Union, 36: 117–160.

Hanks, T.C. and Raleigh, C.B., 1980. The conference on magnitude of deviatoric stresses in the Earth's crust and uppermost mantle. J. Geophys. Res., 85: 6083–6086.

Hanmer, S.K., 1982. Microstructure and geochemistry of plagioclase and microcline in naturally deformed granite. J. Struct. Geol., 4: 197–213.

Hansen, F.D., 1982. Semibrittle creep of selected crustal rocks at 1000 MPa. Ph. D. Thesis, Texas A & M University, College Station, Tex., 224 pp.

Hansen, F.D. and Carter, N.L., 1982. Creep of selected crustal rocks at 1000 MPa. Eos, Trans. Am. Geophys. Union, 63: 437 (Abstr.).

Hansen, F.D. and Carter, N.L., 1983. Semibrittle creep of dry and wet Westerly granite at 1000 MPa. U.S. Symp. on Rock Mechanics, 24th, Texas A & M Univ., College Station, Tex., pp. 429–447.

Hansen, F.D. and Carter, N.L., 1984. Creep of Avery Island Rocksalt. In: R.H. Hardy, Jr. and M. Langer (Editors), The Mechanical Behavior of Salt. Trans. Tech. Publ., Clausthal, pp. 53–69.

Haskell, N.A., 1935. Motions of viscous fluid under a surface load, 1. Physics, 6: 264–269.

Healy, J.H., Rubey, W.W., Griggs, D.T. and Raleigh, C.B., 1968. The Denver earthquakes. Science, 161: 1301–1310.

Heard, H.C., 1972. Steady-state flow in polycrystalline halite at pressures of 2 kilobars. Geophys. Monogr., Am. Geophys. Union, 16: 191–210.

Heard, H.C., 1976. Comparisons of the flow properties of rocks at crustal conditions. Philos. Trans. R. Soc. London, Ser. A, 283: 173–186.

Heard, H.C. and Raleigh, C.B., 1972. Steady-state flow in marble at 500° to 800°C. Geol. Soc. Am. Bull., 83: 935–956.

Hobbs, B.E., 1981. The influence of metamorphic environment upon the deformation of minerals. Tectonophysics, 78: 335–383.

Hobbs, B.E., 1983. Constraints on the mechanism of deformation of olivine imposed by defect chemistry. Tectonophysics, 92: 35–69.

Hobbs, B.E., 1984. Point defect chemistry of minerals under a hydrothermal environment. J. Geophys. Res., 89: 4026–4038.

Hobbs, B.E., Ord, A. and Teyssier, C., 1987. Earthquakes in the ductile regime? Pure Appl. Geophys., in press.

Hoek, E. and Brown, E.T., 1980. Underground excavations in rock. Inst. Min. Metall., London, pp. 95–101.

Jackson, J. and McKenzie, D., 1983. The geometrical evolution of normal fault systems. J. Struct. Geol., 5: 471–483.

Jamison, W.R. and Spang, J.H., 1976. Use of calcite twins to infer differential stress. Geol. Soc. Am. Bull., 87: 868–872.

Jaoul, O., Tullis, J. and Kronenberg, A., 1984. The effect of varying water contents on the creep behavior of Heavitree quartzite. J. Geophys. Res., 89: 4298–4312.

Kappmeyer, J. and Wiltschko, D.V., 1984. Quartz deformation in the Marquetta and Republic troughs, Upper Peninsula of Michigan. Can. J. Earth Sci., 21: 793–801.

Karato, S.-I., 1984. Grain-size distribution and rheology of the upper mantle. Tectonophysics, 104: 155–176.

Karato, S.-I., Toriumi, M. and Fujii, T., 1980. Dynamic recrystallization of olivine single crystals during high temperature creep. Geophys. Res. Lett., 7: 649–652.

Karato, S.-I., Paterson, M.S. and FitzGerald, J.D., 1986. Rheology of synthetic aggregates: Influence of grain size and water. J. Geophys. Res., 91: 8151–8176.

Kay, R.W. and Kay, S.M., 1981. The nature of the lower continental crust: inferences from geophysics, surface geology, and crustal xenoliths. Rev. Geophys. Space Phys., 19: 271–298.

Kerrich, R., LaTour, T.E. and Willmore, L., 1984. Fluid participation in deep fault zones: evidence from geological, geochemical and $^{18}O/^{16}O$ relations. J. Geophys. Res., 89: 4331–4343.

Kirby, S.H., 1977. State of stress in the lithosphere: inferences from the flow laws of olivine. Pure Appl. Geophys., 115: 245–258.

Kirby, S.H., 1980. Tectonic stresses in the lithosphere: Constraints provided by the experimental deformation of rocks. J. Geophys. Res., 85: 6353–6363.

Kirby, S.H., 1983. Rheology of the lithosphere. Rev. Geophys. Space Phys., 21: 1458–1487.

Kirby, S.H., 1984. Introduction and digest to the special issue on chemical effects of water on the deformation and strengths of rocks. J. Geophys. Res., 89: 3991–3995.

Kirby, S.H., 1985. Rock mechanics observations pertinent to the rheology of the continental lithosphere and the localization of strain along shear zones. Tectonophysics, 119: 1–27.

Kirby, S.H. and Kronenberg, A.K., 1984. Deformation of clinopyroxenite: evidence for a transition in flow mechanisms and semibrittle behavior. J. Geophys. Res., 89: 3177–3192.

Kirby, S.H. and McCormick, J., 1984. Inelastic properties of rocks and minerals: Strength and rheology. In: R.S. Carmichael (Editor), CRC Handbook of Physical Properties of Rocks, Vol. III. CRC Press, Boca Raton, Fla., pp. 140–280.

Koch, P.S., 1983. Rheology and microstructures of experimentally deformed quartz aggregates. Ph. D. Thesis, Univ. California, Los Angeles, Calif., 464 pp.

Koch, P.S., Christie, J.M. and George, R.P., Jr., 1980. Flow law of "wet" quartzite in the alpha quartz field. Eos, Trans. Am. Geophys. Union, 61: 376 (Abstr.).

Kogan, M.G. and McNutt, M.K., 1987. Isostasy in the USSR

I: Admittance Data. In: K. Fuchs and C. Froidevaus (Editors), The Composition Structure and Dynamics of Lithosphere–Asthenosphere System, Geodynamics Series, Am. Geophys. Union, Washington, D.C., in press.

Kohlstedt, D.L. and Weathers, M.S., 1980. Deformation-induced microstructures, paleopiezometers and differential stresses in deeply eroded fault zones. J. Geophys. Res., 85: 6269–6285.

Kohlstedt, D.L., Goetze, C. and Durham, W.B., 1976. Experimental deformation of single crystal olivine with application to flow in the mantle. In: R.G.J. Strens (Editor), Petrophysics: The Physics and Chemistry of Minerals and Rocks. Wiley, New York, pp. 35–49.

Kranz, R.L., 1983. Microcracks in rocks: A review. Tectonophysics, 100: 449–480.

Kronenberg, A.K. and Shelton, G.L., 1980. Deformation microstructures in experimentally deformed Maryland diabase. J. Struct. Geol., 2: 341–353.

Kronenberg, A. and Tullis, J., 1984. Flow strengths of quartz aggregates: Grain size and pressure effects due to hydrolytic weakening. J. Geophys. Res., 89: 4281–4297.

Kronenberg, A.K., Kirby, S.H., Aines, R.D. and Rossman, G.R., 1986. Solubility and diffusional uptake of hydrogen in quartz at high water pressures: implications for hydrolytic weakening. J. Geophys. Res., 91: 12,723–12,744.

Lachenbruch, A.H. and Sass, J.H., 1973. Thermo-mechanical aspects of the San Andreas. In: Proceedings of the Conference of the Tectonic Problems of the San Andreas Fault. Stanford Univ. Press, Stanford, Calif., pp. 192–205.

Lachenbruch, A.H. and Sass, J.H., 1977. Heat flow in the United States and the thermal regime of the crust. Geophys. Monogr., Am. Geophys. Union, 20: 626–675.

Lambeck, K., 1980. Estimates of stress differences in the crust from isostatic considerations. J. Geophys. Res., 85: 6397–6401.

Leary, P.C., 1985. Near-surface stress and displacement in a layered elastic crust. J. Geophys. Res., 90: 1901–1910.

Lespinasse, M. and Pecher, A., 1986. Microfracturing and regional stress field: a study of the preferred orientations of fluid-inclusion planes in a granite from the Massif Central, France. J. Struct. Geol., 8: 169–180.

Logan, J.M. and Feucht, L.J., 1985. The effects of chemical environment on the frictional properties of quartzose sandstone. Eos, Trans. Am. Geophys. Union, 66: 1101 (Abstr.).

Logan, J.M., Higgs, N.G. and Friedman, M., 1981. Laboratory studies on natural gouge from the U.S. Geological Survey Dry Lake Valley No. 1 Well, San Andreas Fault Zone. Geophys. Monogr., Am. Geophys. Union, 24: 121–134.

Mackwell, S.J., Kohlstedt, D.L. and Paterson, M.S., 1985. The role of water in the deformation of olivine single crystals. J. Geophys. Res., 90: 11,319–11,333.

Mainprice, D.H. and Paterson, M.S., 1984. Experimental studies of the role of water in plasticity of quartzites. J. Geophys. Res., 89: 4257–4270.

McConnell, R.K., 1968. Viscosity of the Earth's mantle. In: R.A. Phinney (Editor), The History of the Earth's Crust. Princeton Univ. Press, Princeton, N.J., pp. 45–57.

McGarr, A., 1980. Some constraints on levels of shear stress in the crust from observations and theory. J. Geophys. Res., 85: 6231–6238.

McGarr, A., 1984. Some applications of seismic source mechanisms studied in assessing underground hazards. In: N.C. Gay and E.H. Wainwright (Editors), Rockbursts and Seismicity in Mines. South African Institute of Mining and Metallurgy, Symp., 6: 199–208.

McKenzie, D. and Jarvis, G., 1980. The conversion of heat into mechanical work by mantle convection. J. Geophys. Res., 85: 6093–6096.

McNutt, M.K., 1980. Implications of regional gravity for state of stress in the Earth's crust and upper mantle. J. Geophys. Res., 85: 6377–6396.

McNutt, M.K., 1983. Influence of plate subduction on isostatic compensation in Northern California. Tectonics, 2: 399–415.

McNutt, M.K. and Kogan, M.G., 1987. Isostasy in the USSR II: Interpretation of Admittance Data. In: K. Fuchs and C. Froidevaux (Editors), The Composition, Structure and Dynamics of Lithosphere–Asthenosphere System. Geodyn. Ser. Am. Geophys. Union, in press.

McNutt, M.K. and Menard, H.W., 1982. Constraints on yield strength in the oceanic lithosphere derived from observations of flexure. Geophys. J.R. Astron. Soc., 71: 363–394.

Meissner, R. and Strehlau, J., 1982. Limits of stresses in continental crust and their relationship to depth–frequency distribution or shallow earthquakes. Tectonics, 1: 73–89.

Mercier, J-C.C., 1977. Natural periodotites: chemical and rheological heterogeneity of the upper mantle. Ph. D. Thesis, SUNY, Stony Brook, N.Y., 669 pp.

Mercier, J-C.C., 1980a. Single-pyroxene thermobarometry. Tectonophysics, 70: 1–37.

Mercier, J-C.C., 1980b. Magnitude of continental lithospheric stresses inferred from rheomorphic petrology. J. Geophys. Res., 85: 6293–6303.

Mercier, J-C.C. and Nicolas, A., 1975. Textures and fabrics of upper mantle periodotites as illustrated by xenoliths from basalts. J. Petrol., 16: 454–487.

Mercier, J-C.C., Anderson, D.A. and Carter, N.L., 1977. Stress in the lithosphere: Inferences from steady-state flow of rocks. Pure Appl. Geophys., 115: 199–226.

Morrow, C.A., Shi, L.P. and Byerlee, J.D., 1984. Permeability of fault gouge under confining pressure and shear stress. J. Geophys. Res., 89: 3193–3200.

Morton, W.H. and Black, R., 1975. Crustal attenuation in Afar. In: A. Pilger, and A. Rosler (Editors), Afar Depression of Ethiopia. Int. Comm. on Geodyn. Sci. Rep., 14: 55–65.

Müller, W.H. and Briegel, U., 1978. The rheological behavior of polycrystalline anhydrite. Eclogae Geol. Helv., 71: 397–407.

Nicolas, A. and Poirier, J.P., 1976. Crystalline Plasticity and Solid State Flow in Metamorphic Rocks. Wiley-Interscience, London, 444 pp.

Nicolas, A., Boudier, F. and Bouchez, J., 1980. Interpretation of peridotite structures from ophiolitic and oceanic environments. Am. J. Sci., 280-A: 192–210.

Olsson, W.A., 1984. A dislocation model of the stress history dependence of frictional slip. J. Geophys. Res., 89: 9271–9280.

Ord, A. and Hobbs, B.E., 1986. Experimental control of the water-weakening effect in quartz. Geophys. Monogr., Am. Geophys. Union, 36: 51–72.

Ord, A. and Hobbs, B.E., 1987. The strength of the continental crust, detachment zones and the development of plastic instabilities. Tectonics, submitted.

Parrish, D.K., Krivz, A.L. and Carter, N.L., 1976. Finite element folds of similar geometry. Tectonophysics, 32: 183–207.

Paterson, M.S., 1978. Experimental Rock Deformation—The Brittle Field. Springer, Berlin, 254 pp.

Paterson, M.S., 1986. The thermodynamics of water in quartz. Phys. Chem. Miner., 13: 245–255.

Paterson, M.S., 1987. Problems in the extrapolation of laboratory rheological data. Tectonophysics, 133: 33–43.

Pfiffner, O.A., 1982. Deformation mechanisms and flow regimes in limestones from the Helvetic zone of the Swiss Alps. J. Struct. Geol., 4: 429–442.

Pfiffner, O.A., 1985. Displacements along thrust faults. Eclogae Geol. Helv., 78: 313–333.

Pfiffner, O.A. and Ramsay, J.G., 1982. Constraints on geological strain rates: arguments from finite-strain states of naturally deformed rocks. J. Geophys. Res., 87: 311–321.

Phakey, P., Dollinger, G. and Christie, J., 1972. Transmission electron microscopy of experimentally deformed olivine crystals. Geophys. Monogr., Am. Geophys. Union, 16: 117–138.

Poirier, J.P., 1985. Creep of Crystals. Cambridge University Press, New York, N.Y., 260 pp.

Poirier, J.P. and Nicolas, A., 1975. Deformation-induced recrystallization due to progressive misorientation of subgrains with special reference to mantle peridotites. J. Geol., 83: 707–720.

Post, R.L., 1973. The flow laws of Mt Burnet dunite. Ph. D. Thesis, Univ. Calif., Los Angeles, Calif., 272 pp.

Post, R.L., 1977. High-temperature creep of Mt. Burnet dunite. Tectonophysics, 42: 75–110.

Raleigh, C.B., 1977. Frictional heating, dehydration and earthquake stress drops. In: Proceedings of Conference II: Experimental studies of rock friction with application to Earthquake prediction. U.S. Geological Survey, Menlo Park, Calif., pp. 291–304.

Raleigh, C.B. and Evernden, J., 1981. Case for low deviatoric stress in the lithosphere. Geophys. Monogr., Am. Geophys. Union, 24: 173–186.

Raleigh, C.B. and Marone, C., 1986. Dilatancy of quartz gouge in pure shear. Geophys. Monogr., Am. Geophys. Union, 36: 1–10.

Raleigh, C.B., Kirby, S.H., Carter, N.L. and Avé Lallemant, H.G., 1971. Slip and the clinoenstatite transformation as competing rate processes in enstatite. J. Geophys. Res., 76: 4011–4022.

Raleigh, C.B., Healy, J.H. and Bredehoeft, J.D., 1972. Faulting and crustal stress at Rangely, Colorado. Geophys. Monogr., Am. Geophys. Union, 16: 275–284.

Ramsay, J.G. and Wood, D., 1973. The geometric effects of volume changes during deformation processes. Tectonophysics, 16: 263–277.

Reiter, M. and Minier, J., 1985. Possible influences of thermal stresses on Basin and Range faulting. J. Geophys. Res., 90: 10,209–10,222.

Ross, J.V. and Nielsen, K.C., 1978. High-temperature flow of wet polycrystalline enstatite. Tectonophysics, 44: 233–261.

Ross, J.V., Avé Lallemant, H.C. and Carter, N.L., 1980. Stress dependence of recrystallized-grain and subgrain size in olivine. Tectonophysics, 70: 39–61.

Ross, J.V., Bauer, S.J. and Carter, N.L., 1983. Effect of the α–β quartz transition on the creep properties of quartzite and granite. Geophys. Res. Lett., 10: 1129–1132.

Rovetta, M.R., Holloway, J.R. and Blacic, J.D., 1986. Solubility of hydroxyl in natural quartz annealed in water at 900 °C and 1.5 GPa. Geophys. Res. Lett., 13: 145–148.

Rutter, E.H., 1983. Pressure solution in nature, theory and experiment. J. Geol. Soc. London, 140: 725–740.

Rutter, E.H., 1986. On the nomenclature of mode of failure transitions in rocks. Tectonophysics, 122: 381–387.

Sakai, T. and Jonas, J.J., 1984. Dynamic recrystallizations, mechanical and microstructural considerations. Acta Metall., 32: 189–209.

Schmid, S.M., Boland, J.N. and Paterson, M.S., 1977. Superplastic flow in finegrained limestone. Tectonophysics, 43: 257–291.

Schmid, S.M., Paterson, M.S. and Boland, J.N., 1980. High temperature flow and dynamic recrystallization in Carrara Marble. Tectonophysics, 65: 245–280.

Scholz, C.H., 1980. Shear heating and the state of stress on faults. J. Geophys. Res., 85: 6174–6184.

Shelton, G.L., 1981. Experimental deformation of single phase and polyphase crustal rocks at high pressures and temperatures. Ph. D. Thesis, Brown Univ., Providence, R.I., 146 pp.

Shelton, G.L. and Tullis, J., 1981. Experimental flow laws for crustal rocks. Eos, Trans. Am. Geophys. Union, 62: 396.

Shelton, G.L., Tullis, J. and Tullis, T.E., 1981. Experimental high temperature and pressure faults. Geophys. Res. Lett., 8: 55–58.

Sherby, O.D. and Burke, P.M., 1968. Mechanical behavior of crystalline solids at elevated temperature. Prog. Met. Sci., 13: 325–390.

Shimamoto, T., 1985a. The origin of large or great thrust-type earthquakes along subducting plate boundaries. Tectonophysics, 119: 37–65.

Shimamoto, T., 1985b. Confining pressure reduction experiments: A new method for measuring frictional strength over a wide range of normal stress. Int. J. Rock Mech. Min. Sci., 22: 227–236.

Shimamoto, T. and Logan, J.M., 1981. Effects of simulated

fault gouge on the sliding behavior of Tennessee sandstone: nonclay gouges. J. Geophys. Res., 86: 2902–2914.

Shimamoto, T. and Logan, J.M., 1987. Velocity-dependent behavior simulated halite shear zones: an analog for silicates: earthquake source mechanics. Geophys. Monogr., Am. Geophys. Union, in press.

Sibson, R.H., 1977. Fault rocks and fault mechanisms, J. Geol. Soc. London, 133: 191–214.

Sibson, R.H., 1982. Fault zone models, heat flow, and depth distribution of earthquakes in the continental crust of the United States. Bull. Seismol. Soc. Am., 72: 151–163.

Sibson, R.H., 1983. Continental fault structure and the shallow earthquake source. J. Geol. Soc. London, 140: 741–767.

Sibson, R.H., 1984. Roughness at the base of the seismogenic zone: contributing factors. J. Geophys. Res., 89: 5791–5799.

Smith, D.L. and Evans, B., 1984. Diffusional crack healing in quartz. J. Geophys. Res., 89: 4125–4135.

Smith, R.B. and Bruhn, R.L., 1984. Intraplate extensional tectonics of the eastern Basin-Range: inferences on structural style from seismic reflection data, regional tectonics, and thermal–mechanical models of brittle–ductile deformation. J. Geophys. Res., 89: 5733–5762.

Smithson, S.B. and Brown, S.K., 1977. A model for lower continental crust. Earth Planet. Sci. Lett., 35: 134–144.

Solomon, S.C., Richardson, R.M. and Bergman, E.A., 1980. Tectonic stress: Models and magnitudes. J. Geophys. Res., 85: 6086–6092.

Stesky, R.M., 1978. Mechanisms of high temperature frictional sliding in Westerly granite. Can. J. Earth Sci., 15: 361–375.

Stesky, R.M., Brace, W.F., Riley, D.K. and Robin, P.-Y.F., 1974. Friction in faulted rock at high temperature and pressure. Tectonophysics, 23: 177–203.

Stocker, R.L. and Ashby, M.F., 1973. On the rheology of the upper mantle. Rev. Geophys. Space Phys., 11: 391–426.

Taylor, H.P., Jr., 1977. Water/rock interaction and the origin of H_2O in granitic batholiths. J. Geol. Soc. London, 133: 509–588.

Tsenn, M.C. and Carter, N.L., 1987. Upper limits of power law creep in rocks. Tectonophysics, 136: 1–26

Tullis, J., 1979. High temperature deformation of rocks and minerals. Rev. Geophys. Space Phys., 17: 1137–1154.

Tullis, J. and Yund, R.A., 1977. Experimental deformation of dry Westerly granite. J. Geophys. Res., 82: 5705–5718.

Tullis, J. and Yund, R.A., 1980. Hydrolytic weakening of experimentally deformed Westerly granite and Hale albite rock. J. Struct. Geol., 2: 439–451.

Tullis, J. and Yund, R.A., 1985. Dynamic recrystallization of feldspar: A mechanism for ductile shear zone formation. Geology, 13: 238–241.

Tullis, J., Shelton, G.L. and Yund, R.A., 1979. Pressure dependence of rock strength: implications for hydrolytic weakening. Bull. Mineral., 102: 110–114.

Tullis, T.E., 1980. The use of mechanical twinning in minerals as a measure of shear stress magnitudes. J. Geophys. Res., 85: 6263–6268.

Tullis, T.E. and Horowitz, F.G., 1980. The strength of dry olivine. Eos, Trans. Am. Geophys. Union, 61: 375–376 (Abstr.).

Tullis, T.E. and Horowitz, F.G., 1987. The strength of dry olivine. J. Geophys. Res., in press.

Tullis, T.E. and Tullis, J., 1986. Experimental rock deformation techniques. Geophys. Monogr., Am. Geophys. Union, 36: 297–324.

Turcotte, D.L., Tag, P.H. and Cooper, R.F., 1980. A steady state model for the distribution of stress and temperature on the San Andreas Fault. J. Geophys. Res., 85: 6224–6230.

Twiss, R.J., 1977. Theory and applicability of a recrystallized grain size paleopiezometry. Pure Appl. Geophys., 115: 227–244.

Twiss, R.J., 1986. Variable sensitivity piezometric equations for dislocation density and subgrain diameter and their relevance to olivine and quartz. Geophys. Monogr., Am. Geophys. Union, 36: 247–262.

Urai, J.L., Means, W.D. and Lister, G.S., 1986. Dynamic recrystallization of minerals. Geophys. Monogr., Am. Geophys. Union, 36: 161–199.

Von Karman, T., 1911, Festigkeitsversuche unter allseitigem Druck. Z. Ver. Dtsch. Ing., 55: 1749–1757.

Walcott, R.I., 1970. Flexural rigidity thickness and viscosity of the lithosphere. J. Geophys. Res., 75: 3941–3954.

Wang, C., Mao, N. and Wu, F.T., 1980. Mechanical properties of clays at high pressure. J. Geophys. Res., 85: 1462–1468.

Watts, A.B., Bodine, J.H. and Steckler, M.S., 1980. Observations of flexure and the state of stress in the oceanic lithosphere. J. Geophys. Res., 85: 6369–6376.

Wawersik, W.R. and Hannum, D.W., 1979. Interim summary of Sandia creep experiments on rock salt from the WLPP study area, southeastern New Mexico. DOE Contract DG-AC04-760DP0079.

Weeks, J.D. and Tullis, T.E., 1985. Frictional sliding of dolomite: A variation in constitutive behavior. J. Geophys. Res., 90: 7821–7826.

Weertman, J., 1968. Dislocation climb theory of steady-state creep. Trans. ASME, 61: 681–694.

Weertman, J., 1978. Creep laws for the mantle of the Earth. Philos. Trans. R. Soc. London, Ser. A, 288: 9–26.

Weertman, J. and Weertman, J.R., 1975. High temperature creep of rock and mantle viscosity. Annu. Rev. Earth Planet. Sci., 3: 293–315.

Weertman, J. and Weertman, J.R., 1983. Mechanical properties, strongly temperature-dependent. In: R.W. Cahn and P. Haasen (Editors), Physical Metallurgy. Elsevier, New York, pp. 1310–1340.

Weidner, D.J., 1985. A mineral physics test of a pyrolite mantle. Geophys. Res. Lett., 12: 417–420.

Wernicke, B. and Burchfiel, B.C., 1982. Modes of extensional tectonics. J. Struct. Geol., 4: 105–115.

White, J.C. and White, S.H., 1983. Semi-brittle deformation within the Alpine fault zone, New Zealand. J. Struct. Geol., 5: 579–589.

White, S., 1979a. Paleo-stress estimates in the Moine Thrust zone, Eriboll, Scotland. Nature, 280: 222–223.

White, S., 1979b. Grain and sub-grain size variations across a mylonite zone. Contrib. Mineral. Petrol., 70: 193–202.

Whitten, C.A., 1956. Crustal movements in California and Nevada. Eos, Trans. Am. Geophys. Union, 37: 393.

Wilks, K.R. and Carter, N.L., 1986. High temperature creep of layer 3 gabbros of the Zambales ophiolite. 99th Geol. Soc. Am. Annu. Meet., p. 789 (Abstr.).

Yund, R.A. and Tullis, J., 1980. The effect of water, pressure, and strain on Al/Si order–disorder kinetics in feldspar. Contrib. Mineral. Petrol., 72: 297–302.

Zeuch, D.H., 1982. Ductile faulting, dynamic recrystallization and grain-size-sensitive flow of olivine. Tectonophysics, 83: 293–308.

Zeuch, D.H., 1983. On the inter-relationship between grain size sensitive creep and dynamic recrystallization of olivine. Tectonophysics, 93: 151–168.

Zeuch, D.H. and Green, H.W., II, 1984a. Experimental deformation of a synthetic dunite of high temperature and pressure. I. Mechanical behavior, optical microstructure and deformation mechanism. Tectonophysics, 110: 233–262.

Zeuch, D.H. and Green, H.W., II, 1984b. Experimental deformation of a synthetic dunite at high temperature and pressure. II. Transmission electron microscopy. Tectonophysics, 110: 263–296.

Zoback, M.D. and Mastin, L., 1986. Implications of wellbore breakouts for the state of stress at mid-crustal depths in the Kola Peninsula ultradeep borehole. Eos, Trans. Am. Geophys. Union, 67: 382.

Zoback, M.D., Tsukahara, H. and Hickman, S., 1980. Stress measurements at depth in the vicinity of the San Andreas fault: implications for the magnitude of shear stress at depth. J. Geophys. Res., 85: 6157–6173.

Zuber, M.T., Parmentier, E.M. and Fletcher, R.C., 1986. Extension of continental lithosphere: A model for two scales of Basin and Range deformation. J. Geophys. Res., 91: 4826–4838.